

Applications of PIP -Pyrrole-Imidazole Polyamide-

Literature seminar #1

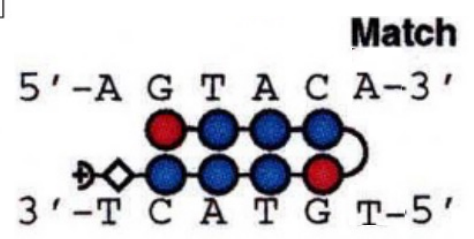
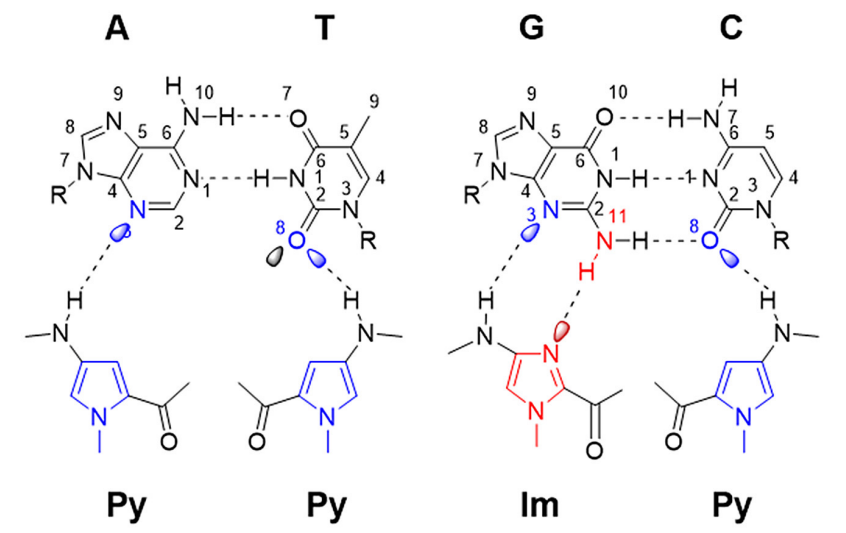
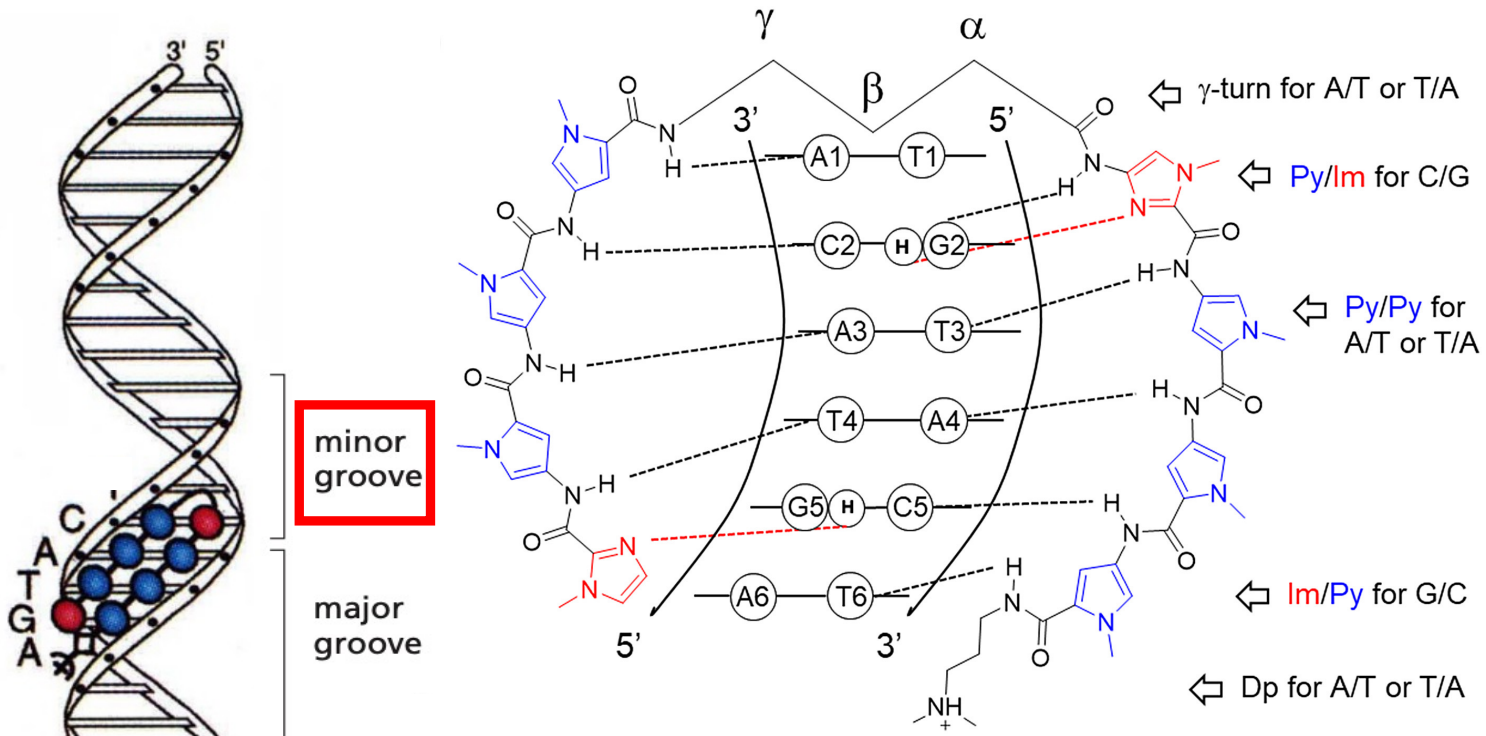
2024/1/25

B4 Mayo Yamazaki

- Introduction
- KR12 (DNA alkylating agent with PIP)
- Bi-PIP (Brd inhibitor with PIP)
- PIP-HoGu (Integration of PIP and cooperative systems)
- ePIP-HoGu (PIP-HoGu with epigenetic modulator)
- Summary & Discussion

- Introduction
- KR12 (DNA alkylating agent with PIP)
- Bi-PIP (Brd inhibitor with PIP)
- PIP-HoGu (Integration of PIP and cooperative systems)
- ePIP-HoGu (PIP-HoGu with epigenetic modulator)
- Summary & Discussion

What is PIP (pyrrole-imidazole polyamide)?

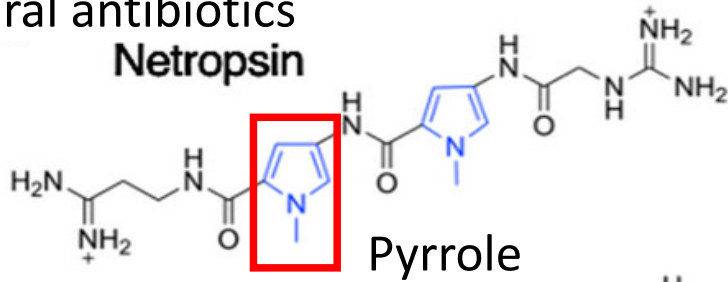


- ✓ PIP is a programmable DNA minor groove binder.
- ✓ PIP selectively recognizes the four base pairs in duplex DNA.
 - Im/Py pair → G/C base pair
 - Py/Py pair → A/T or T/A base pair
- ✓ $K_d < 1$ nM (similar to DNA-binding proteins)

A Brief History of PIP

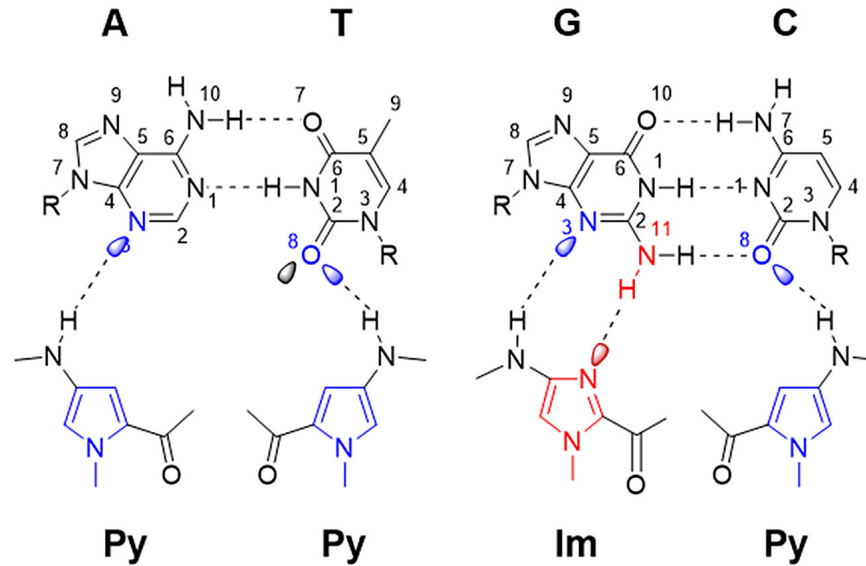
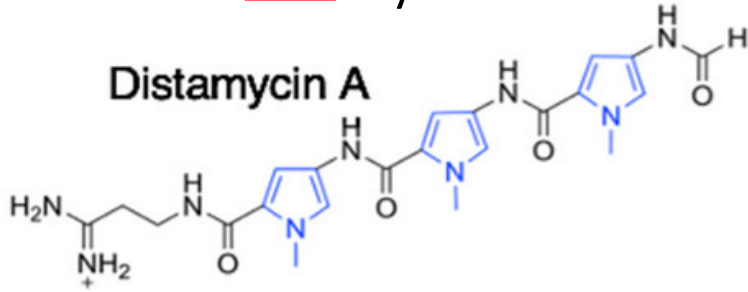
Natural antibiotics

Netropsin



Pyrrole

Distamycin A



- ✓ Netropsin binds to A/T sequences in the DNA minor groove by forming a 1:1 complex. (1985)

Dickerson, R. E. *et al. J. Mol. Biol.* **1985**, *183*, 553–563

- ✓ Distamycin A binds to A/T sequences in the DNA minor groove by forming 2:1 complex. (1989)

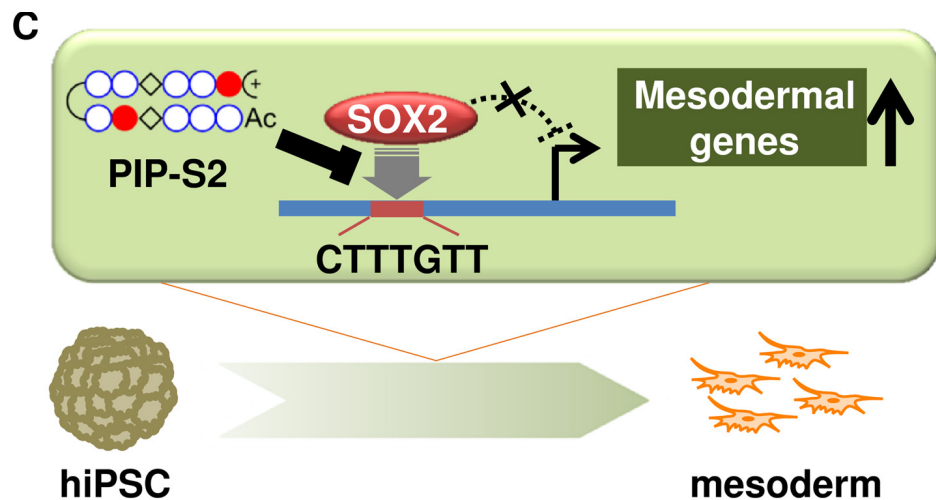
Wemmer, D. E. *et al. Proc. Natl. Acad. Sci. U.S.A.* **1989**, *86*, 5723–5727

- ✓ Replacing Py with Im enabled the recognition of G/C sequences.

Dickerson, R. E. *et al. Proc. Natl. Acad. Sci. U.S.A.* **1985**, *82*, 1376–1380

Applications of PIPs

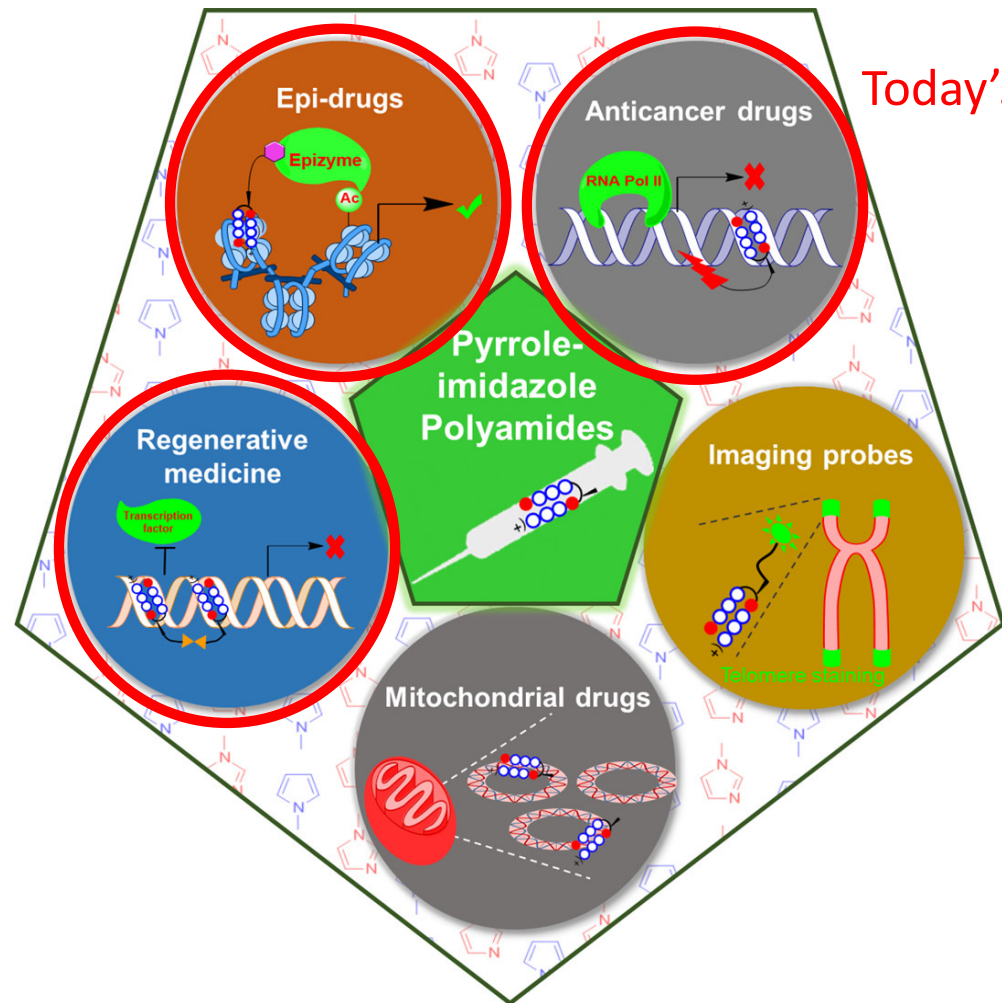
ex) Single PIP can inhibit transcription factor



- Designing PIP to bind to SOX2 target sequence
- The PIP inhibited SOX2 and promoted the transcription of Mesodermal genes

Taniguchi, J., Sugiyama, H. *et al. Nucleic Acids Res.* **2017**, *45*, 9219–9228

Variety of applications of PIP

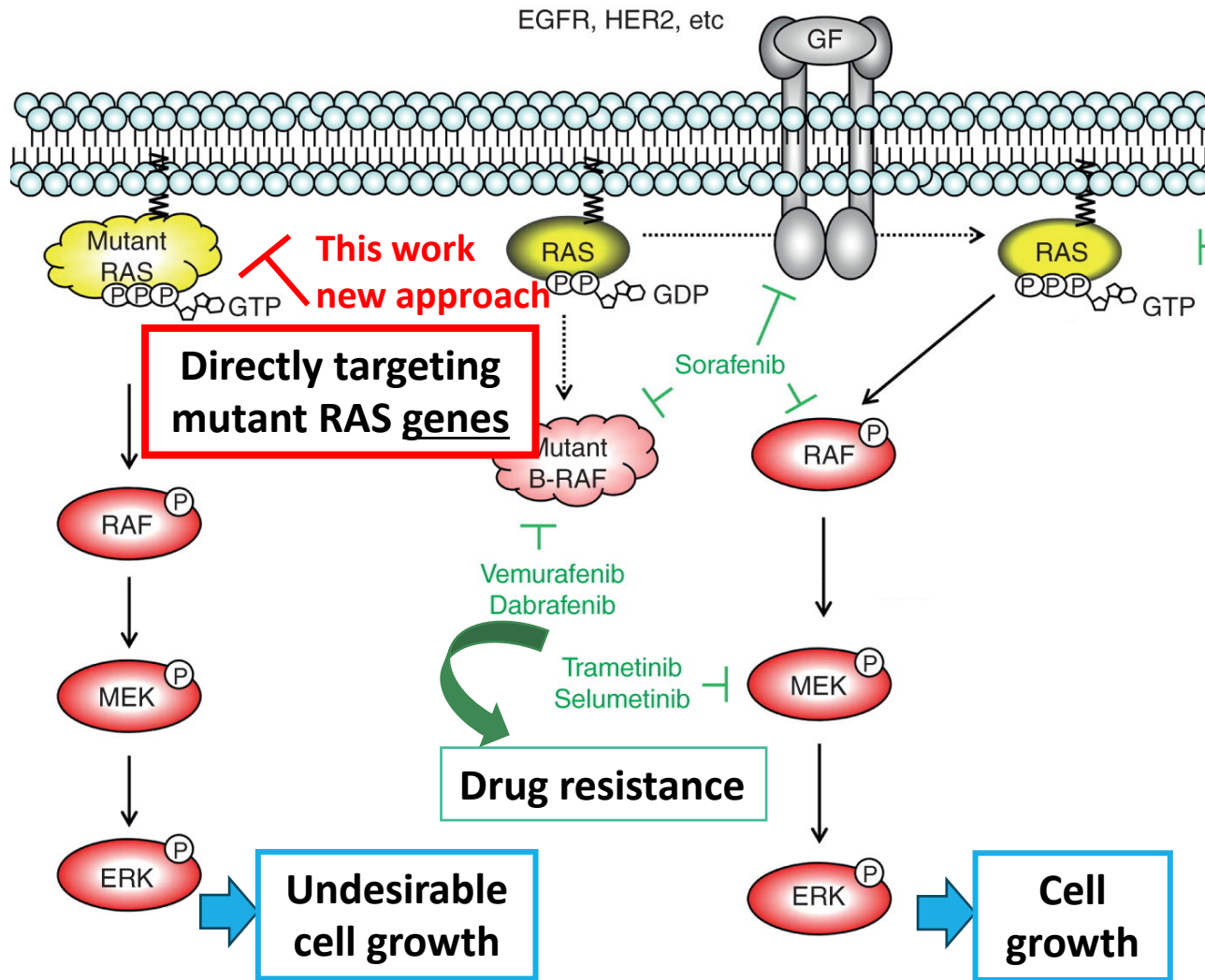


Today's topic

- Introduction
- KR12 (DNA alkylating agent with PIP)
- Bi-PIP (Brd inhibitor with PIP)
- PIP-HoGu (Integration of PIP and cooperative systems)
- ePIP-HoGu (PIP-HoGu with epigenetic modulator)
- Summary & Discussion

A novel approach directly targeting the mutant DNA

KR12



Takashima, A. *et al. Expert Opin. Ther. Targets.* **2013**, *17*, 507-531

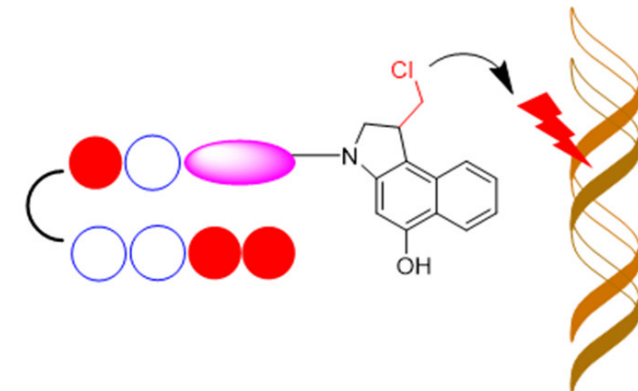
- Oncogenic driver mutations = Target for therapy

ex) KRAS mutation

- Many colon cancer patients have the **KRAS (G12D) mutation or the (G12V) mutation.**

- Direct pharmacological targeting of activated KRAS has **not** led to clinical application.

- ✓ Development of **PIP-indole-seco-CBI conjugates** targeting KRAS codon 12 mutations

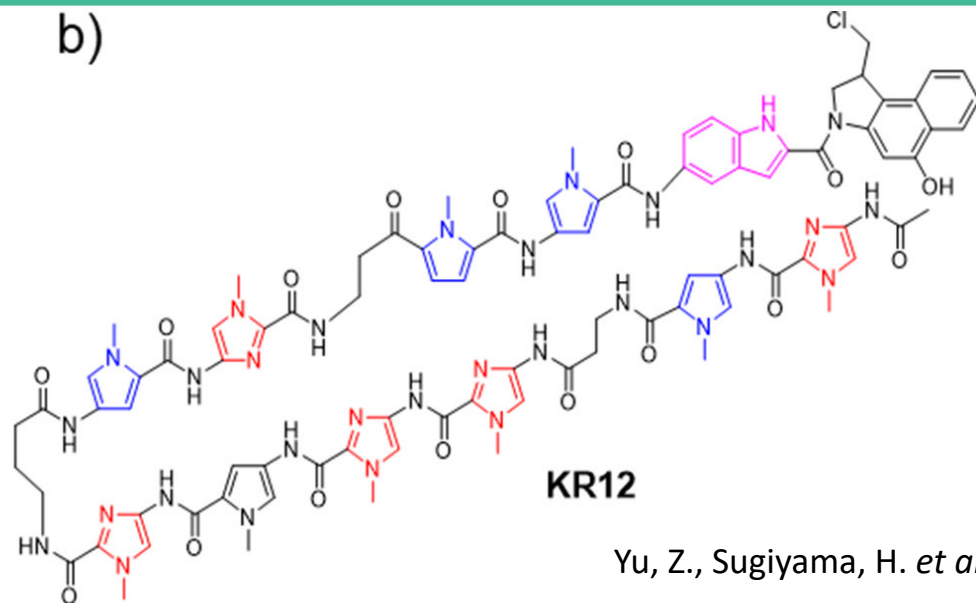


Yu, Z., Sugiyama, H. *et al. Adv. Drug Delivery Rev.* **2019**, *147*, 66-85 2024/1/25

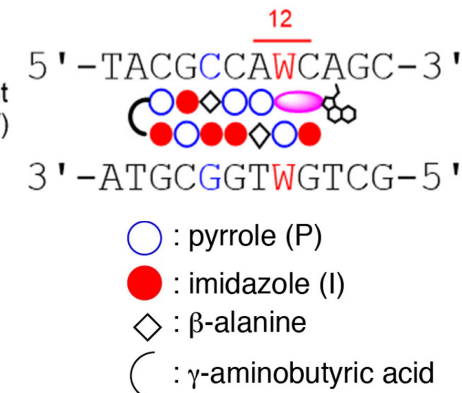
KR12 targets KRAS codon 12 (G12D and G12V) mutants



b)



KRAS mutant
 (G12D;G12V)
 W=A/T



Yu, Z., Sugiyama, H. *et al. Adv. Drug Delivery Rev.* **2019**, *147*, 66-85

Summary table of the dissociation constants

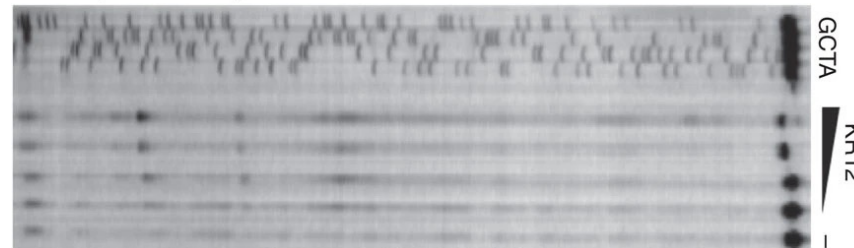
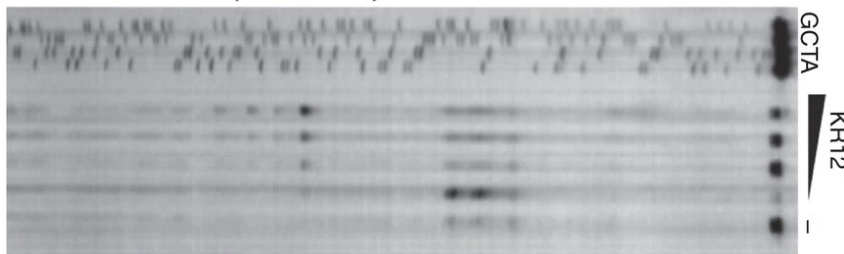
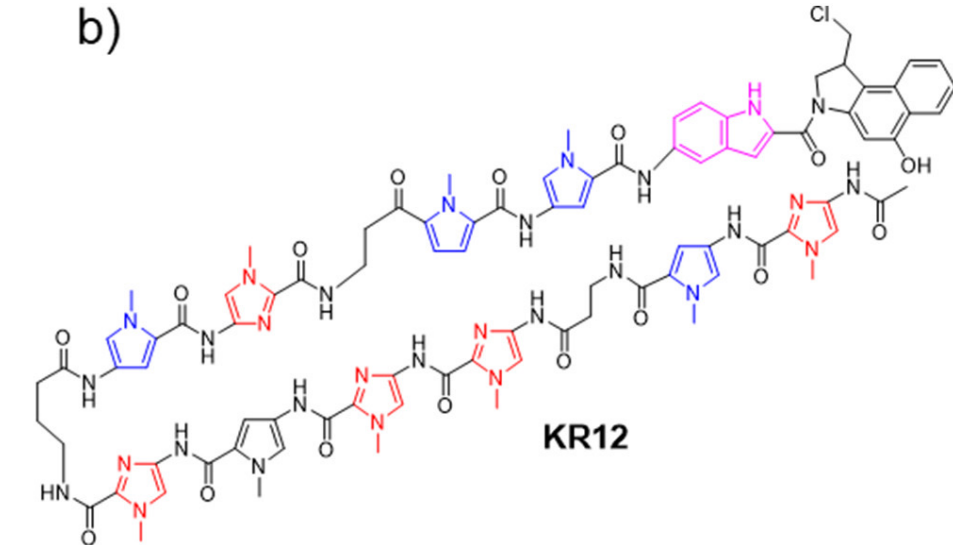
PI-Polyamide	Sequence	KD(10 ⁻⁹ M)
KR12-Dp	WT(GGT)	114.0
	MUT(GAT)	8.5
	MUT(GTT)	17.1

✓ KR12 preferentially bound to **the mutant KRAS sequences** compared to the wild type.

KR12 alkylated at mutated KRAS codon 12 sites

KR12

- Thermally induced strand cleavage procedure
- ✓ Dose-dependent alkylation by KR12 was detected only at the mutated KRAS codon 12 target sites

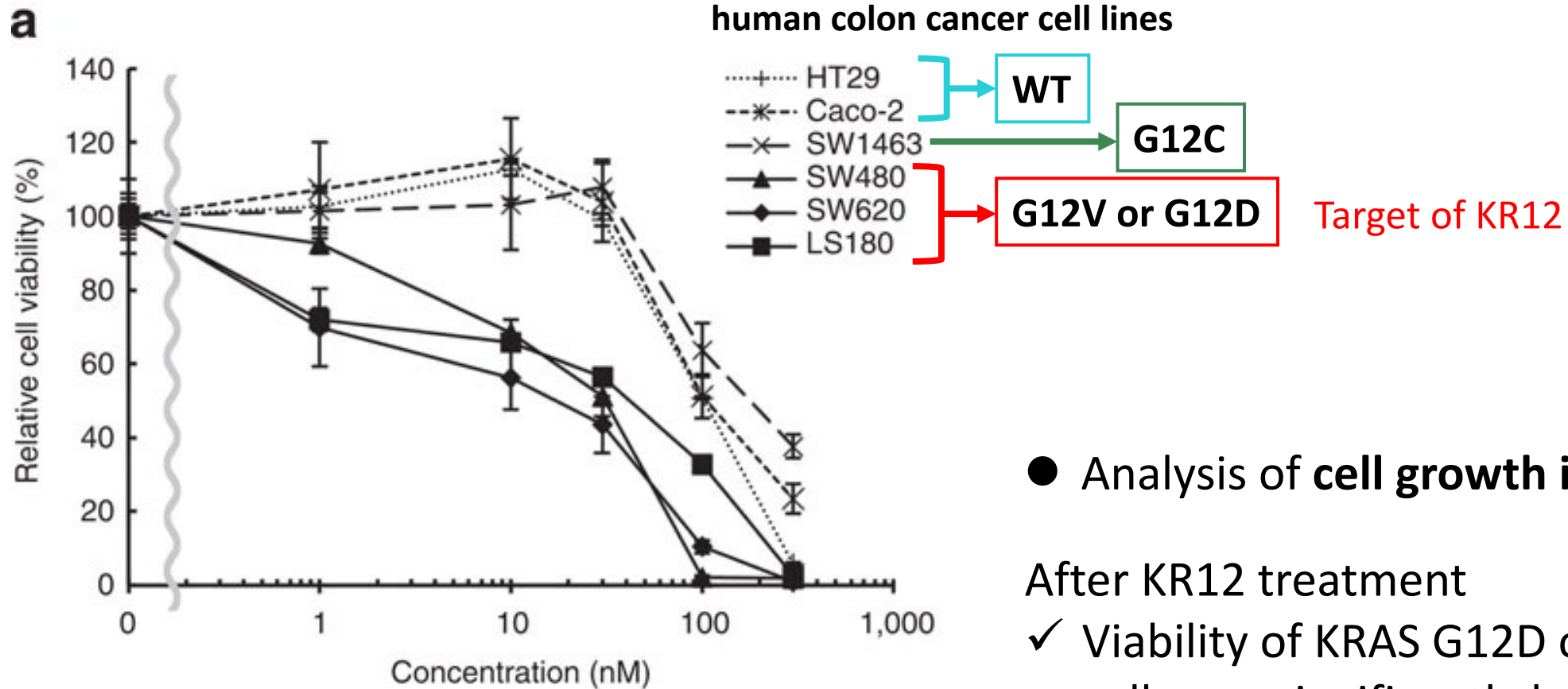


DNA alkylation was visualized by thermal cleavage of the 5'-Texas Red labeled DNA strands at the alkylated sites, which displayed cleavage bands quantitatively on the polyacrylamide gel.

5'-Texas Red-labelled DNA fragments containing the indicated KRAS codon 12 mutations were incubated with the indicated concentrations of KR12 for 10 h at room temperature, followed by the addition of calf thymus DNA. The reaction mixtures were then incubated at 90 ° C for 5 min to cleave DNA strands at their specific alkylated sites. DNA fragments were then recovered by vacuum centrifugation, dissolved in loading dye, denatured at 95 ° C for 20 min and subjected to electrophoresis on a 6% denaturing polyacrylamide gel.

2024/1/25

KR12 inhibited cell growth of KRAS mutated human cancer cell



- Analysis of cell growth inhibition by KR12

After KR12 treatment

- ✓ Viability of KRAS G12D or G12V mutant cells was significantly lower

Figure 2 | KR12-mediated specific suppression of KRAS codon 12 mutants in human colon cancer cells. (a) WST assay. Human colon cancer cells expressing wild-type KRAS, including HT29 and Caco-2 or human colon cancer cells harbouring KRAS codon 12 mutations, including SW1463, SW480, SW620 and LS180, were incubated with the indicated concentrations of KR12. 48 hours after treatment, the percent viable cells were examined by WST assay and depicted in a line graph. Error bars indicate the s.d. of the data from triplicate experiments.

KR12 induced mutant KRAS suppression

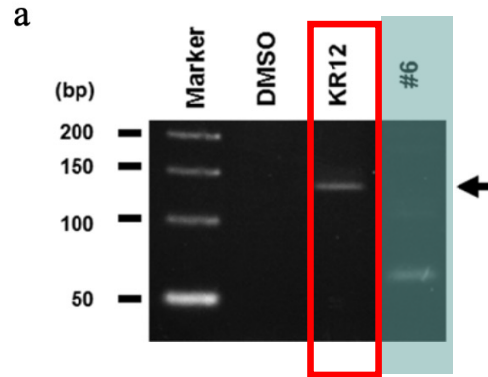
Analysis of the specific alkylation and subsequent downregulation after KR12 treatment

KR12

Human colon cancer-derived, heterozygously mutated LS180 (12D/WT) cells

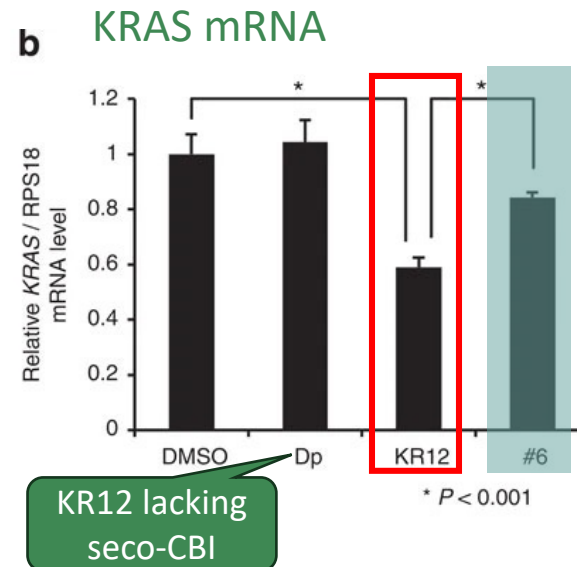
In Cell

Endogenous alkylation confirmed by
Ligation-mediated PCR



✓ KR12 induced DNA
alkylation in LS180 cells.

#6 = not bound to the codon 12 mutant KRAS sequences



(b) Quantitative reverse transcription-PCR analysis. Relative KRAS expression **48 h** after treatment with DMSO, KR12, #6 or Dp was plotted as a bar graph. Error bars indicate the s.d. of data from triplicate experiments. (d) Immunoblot analysis. Immunoblots for anti-KRAS or anti-actin antibody (top and bottom panels, respectively) for LS180 (12D/WT) and HT29 (WT) cells **48 h** after the treatment with either control DMSO solution, KR12 or #6. The GST-Raf-bound proteins from each treated group were pulled down and analysed by immunoblotting with anti-RAS antibody (middle panels).

KRAS protein



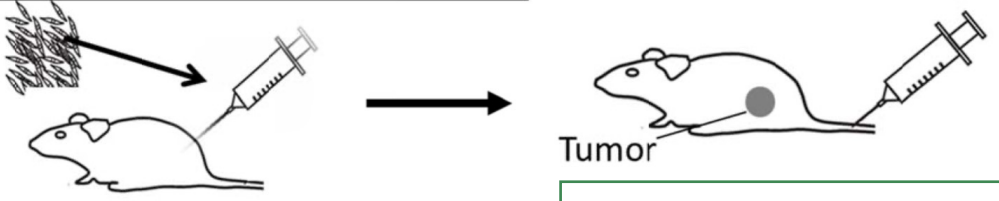
- ✓ Significant downregulation of total KRAS RNA
- ✓ Specific reductions in activated KRAS protein levels in LS180 cells

2024/1/25

KR12 showed tumor growth reduction *in vivo*

HT29 (2×10^6 cells), LS180 (3×10^6 cells) or SW480 (5×10^6 cells) were subcutaneously injected into the right thigh of six-week-old athymic female mice. Mice were inoculated with cells and allowed to reach tumor volumes between 50 to 100 mm³.

Once a week tail vein injection of KR12 (320 µg/kg) or 1.25% DMSO solution for 5 weeks was performed.



White = Control (DMSO)
Black = KR12-treated group

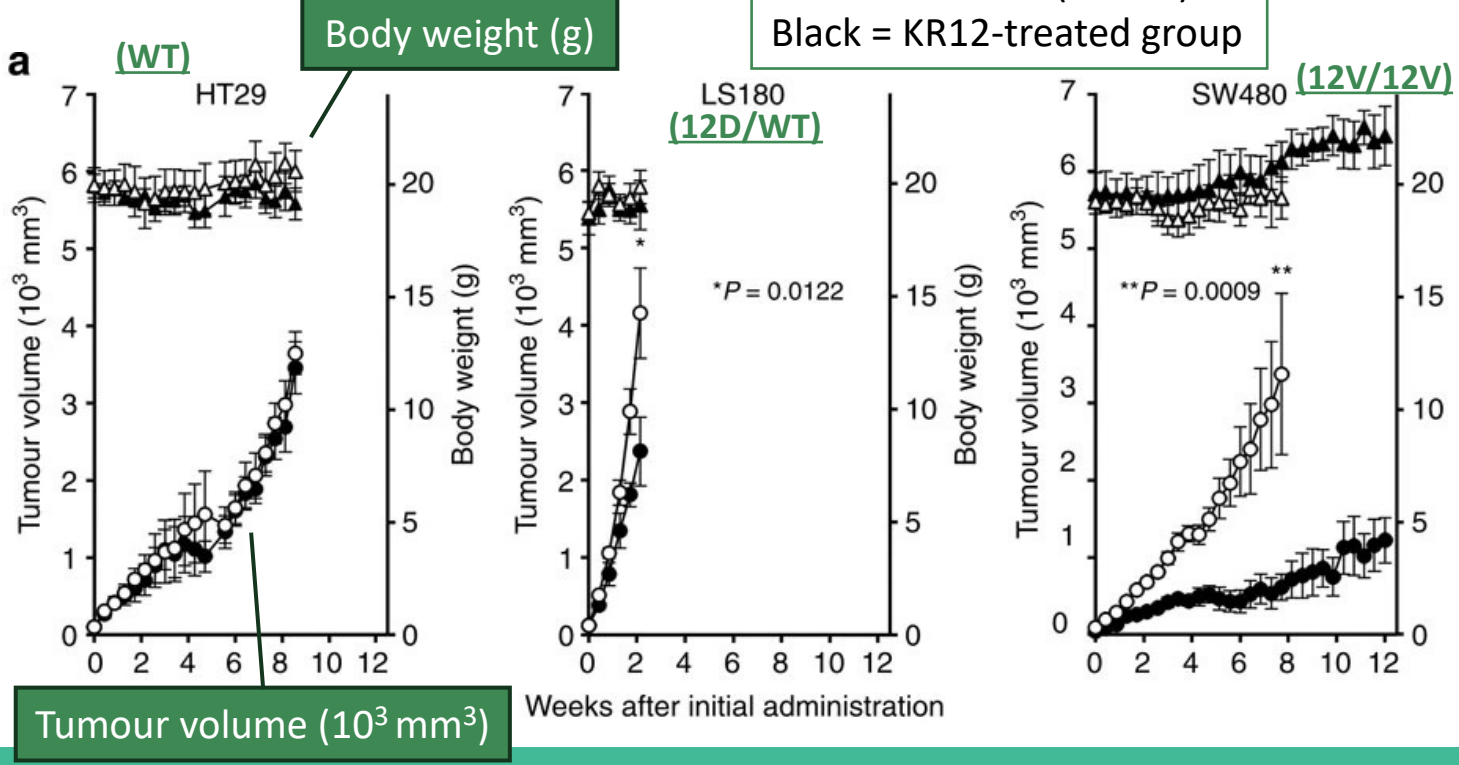


Figure 4 | KR12 suppresses tumour growth *in vivo*. (a) The indicated human colon cancer cells, that is, HT29 (WT), LS180 (12D/WT) and SW480 (12V/12V), were injected subcutaneously into BALB/c nude mice. When the tumour volume reached 100 mm³, DMSO or KR12 (320 mg kg⁻¹ body weight) was intravenously injected through the tail vein every 7 days. At the indicated times after administration, the tumour volume was calculated as 1/6 π the longest diameter width height. The mean tumour volume, with s.e. (open circles for DMSO and closed circles for KR12 treatment), and mean body weight, with s.e. (open triangles for DMSO and closed triangles for KR12 treatment), of the KR12-treated group and control group are plotted in a line graph with error bars (s.e.). The numbers of animals used were 6 for HT29 (DMSO and KR12) and LS180 (KR12), 5 for LS180 (DMSO) and SW480 (KR12), and 8 for SW480 (DMSO). (b) Images of the euthanized mice of each group are shown. An image of an SW480 xenograft 5 weeks after KR12 treatment, which was the final treatment, is also shown.

KR12-treated LS180 and SW480
 ✓ Significant reduction of tumor growth with minimum toxicity

KR12 showed lower toxicity than CBI without PIP

KR12

In Cells

cell lines with KRAS mutations recognized by KR12

Cell lines	KRAS status	KRAS	P53 status	KR12 IC50(nM)	CBI IC50(nM)
SW480	MUT	G12V	MUT	31	10
SW620	MUT	G12V	MUT	17	10
SNU-C2B	MUT	G12D	MUT	57	18
LS180	MUT	G12D	WT	42	17
SW1463	MUT	G12C	MUT	178	20
DLD-1	MUT	G13D	MUT/WT	153	13
HT-29	WT	WT	MUT	102	25
Caco-2	WT	WT	MUT	105	18

- CBI itself treatment

- In cells

IC50 did **not** change depending on KRAS codon 12 mutant.

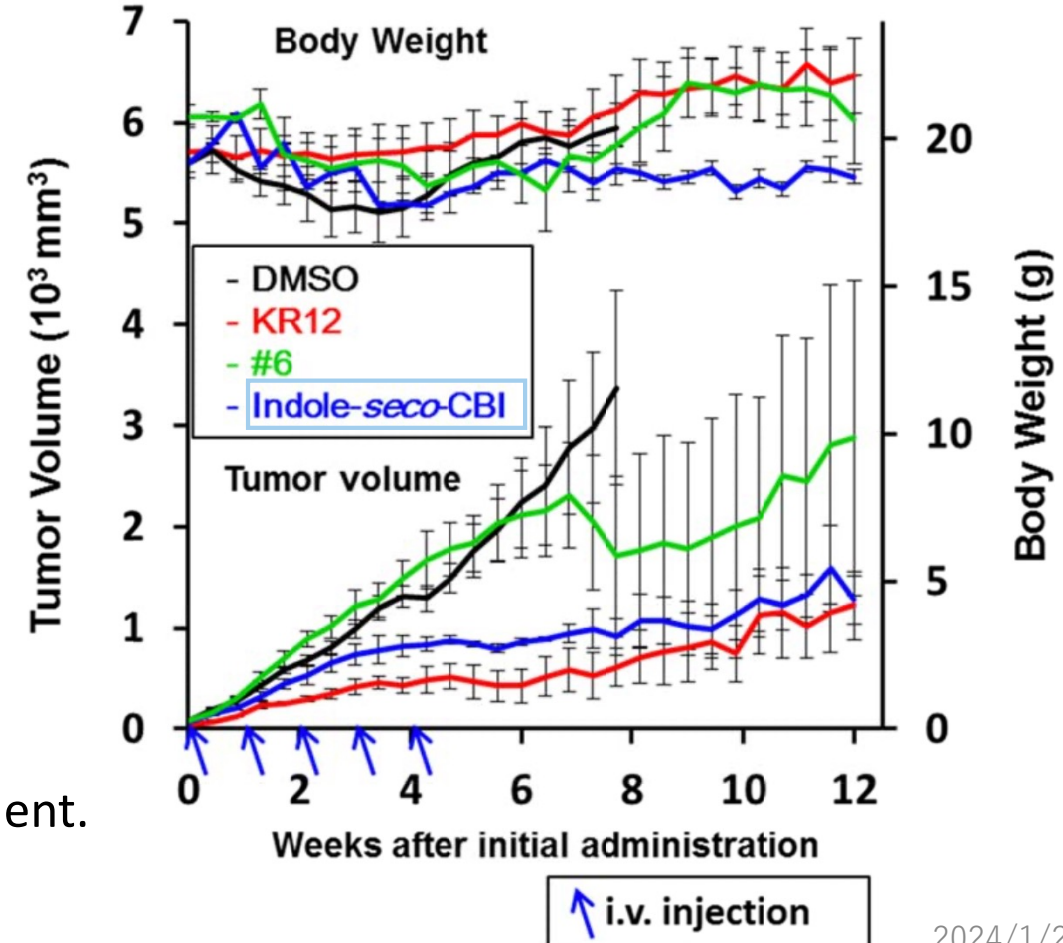
- In vivo

Tumour growth reduction was slightly **weaker** than KR12 treatment.

Mice showed **weight loss** and **slight illness**.

In vivo

SW480 (G12V/G12V)



Summary of KR12 & Challenges

Summary

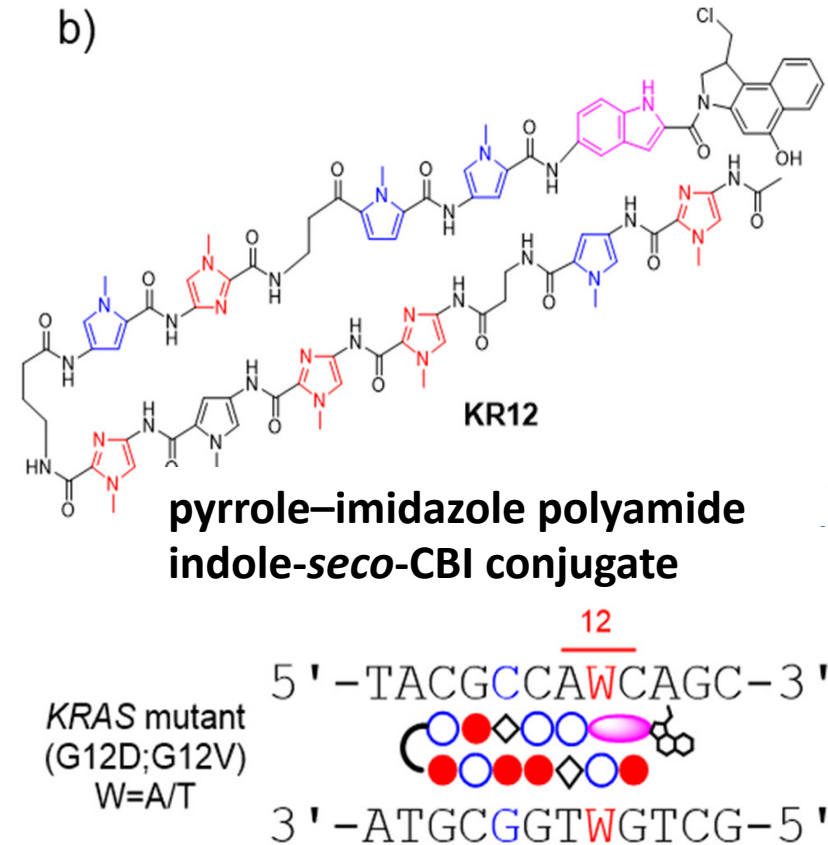
KR12...

- ✓ alkylated mutant DNA sequence selectively.
- ✓ downregulated active KRAS.
- ✓ suppressed the growth of KRAS G12V/G12D mutant tumor *in vivo*.
- ✓ reduced the toxicity of the alkylating agent.
- ✓ produced effects that were not achieved by PIP alone or the DNA alkylating agent alone.

Challenges

- Optimization to improve their specificity
- 9,121 target sites = Potential off-target of KR12

KR12



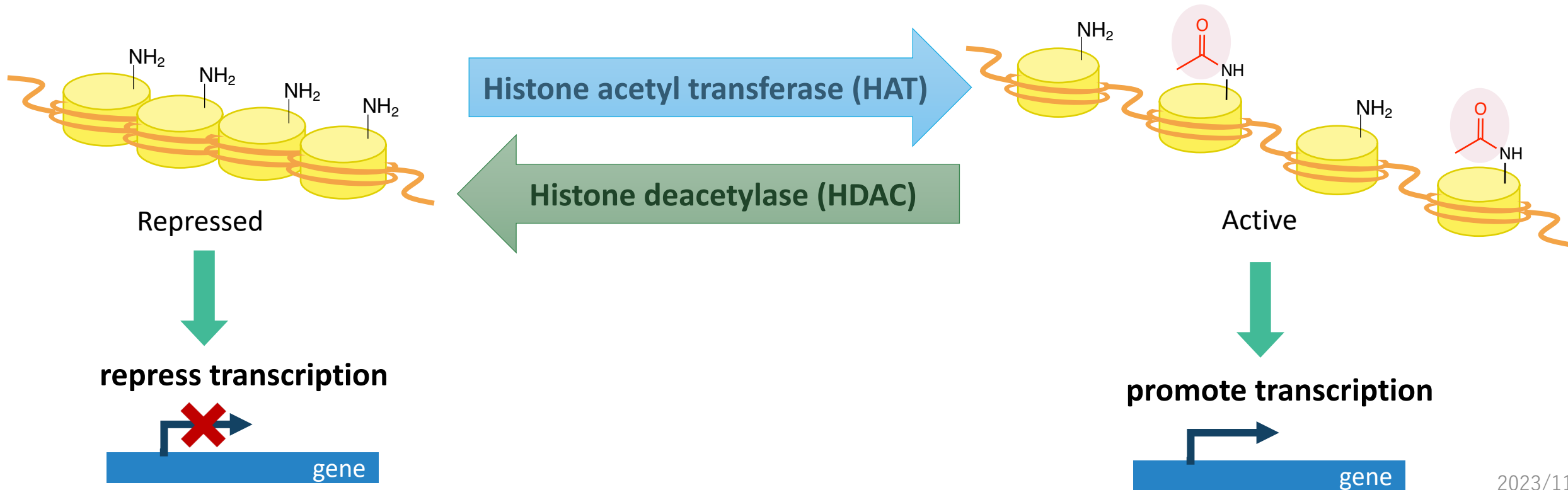
Yu, Z., Sugiyama, H. *et al.* *Adv. Drug Delivery Rev.* **2019**, 147, 66-85

- Introduction
- KR12 (DNA alkylating agent with PIP)
- **Bi-PIP (Brd inhibitor with PIP)**
- PIP-HoGu (Integration of PIP and cooperative systems)
- ePIP-HoGu (PIP-HoGu with epigenetic modulator)
- Summary & Discussion

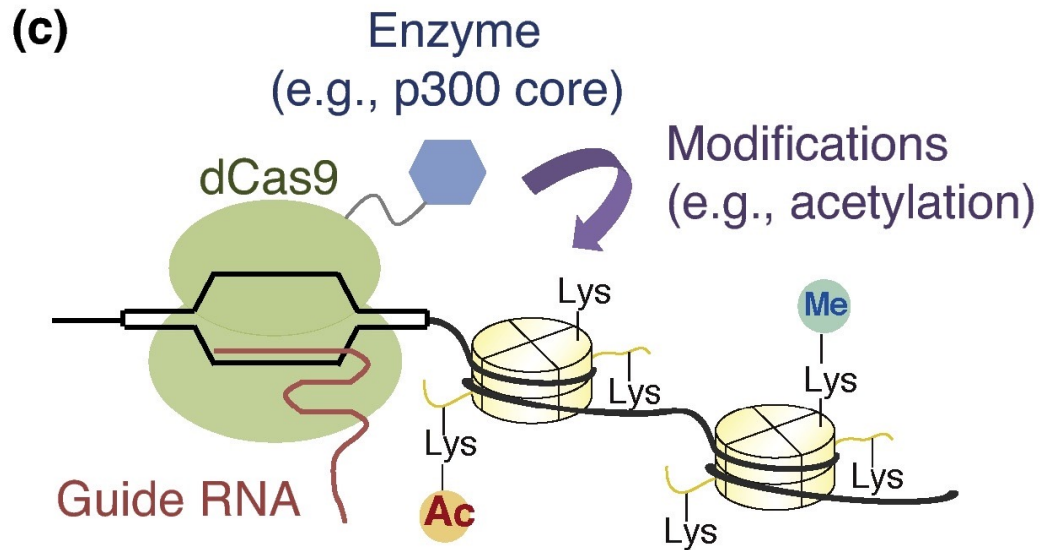
Acetylation of histone lysine residues regulates transcription

Acetylation of histone lysine residues is strongly correlated with transcriptional activation.

- opening the chromatin structure
- recruiting proteins containing bromodomain (BD)



Previous design to achieve sequence-selective histone acetylation

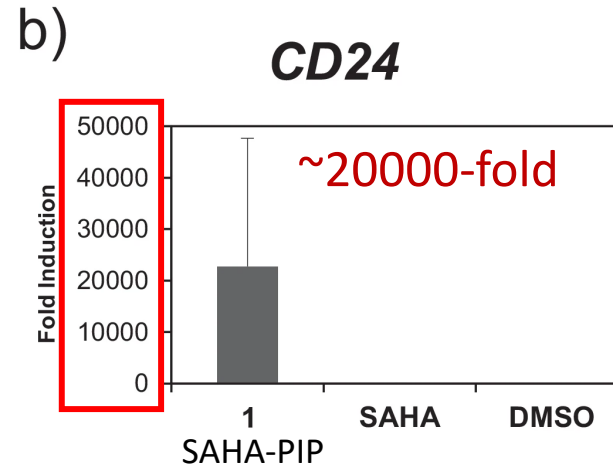


Recent

- fusion of P300 (containing HAT) with CRISPR/Cas system
- ✗ need the **transfection**-based system
- ✗ enzymatic **degradation** in cell

Hilton, I., Gersbach, C. *et al. Nat. Biotechnol.* **2015**, *33*, 510–517

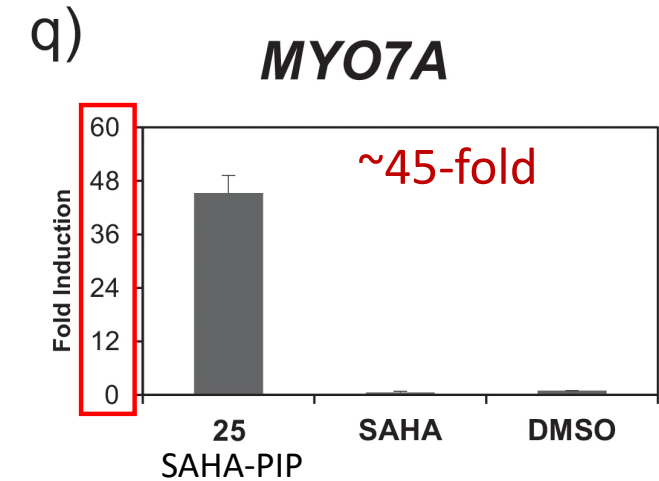
Yamatsugu, Kawashima, Kanai *Curr. Opin. Chem. Biol.* **2018**, *46*, 10–17



Previous effort using PIP

- SAHA (HDAC inhibitor) –PIP
- **inconsistent** of the level of gene activation **because of indirect manner**

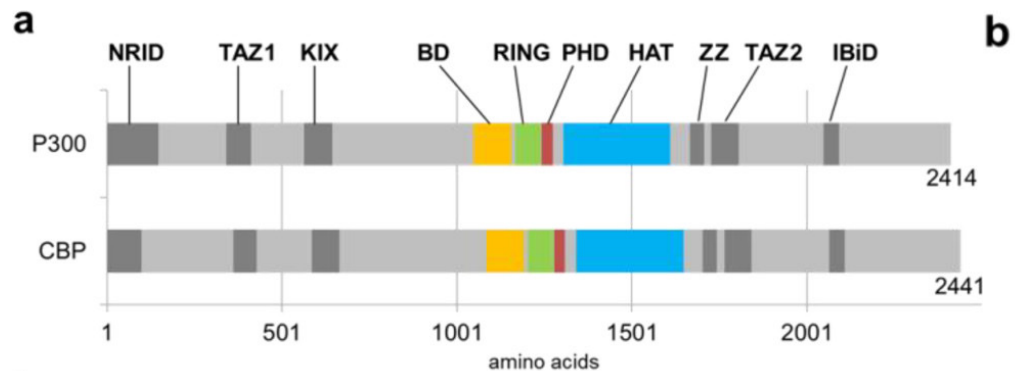
Pandian, GN., Sugiyama, H. *et al. Sci. Rep.* **2014**, *4*, 3843



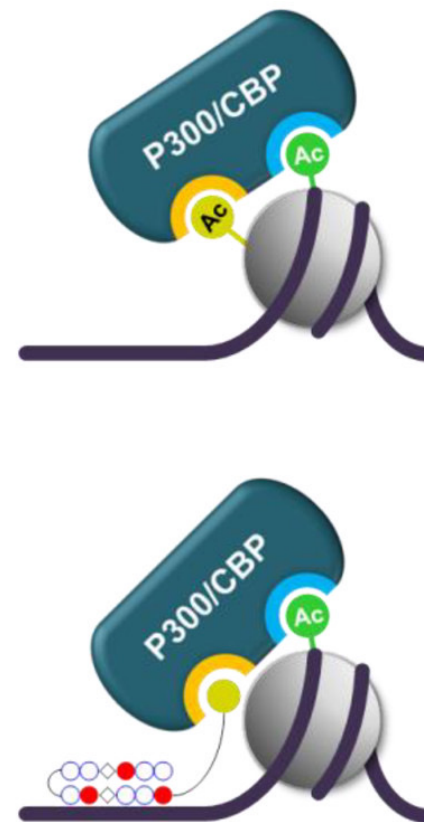
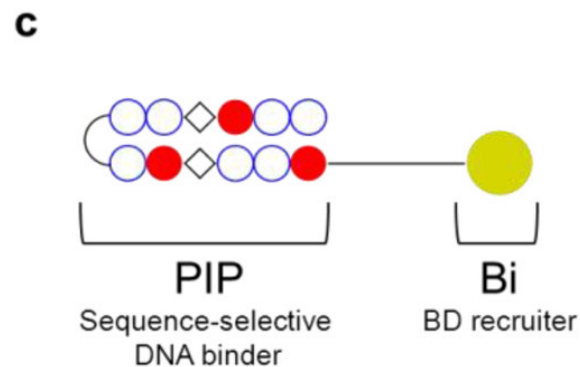
Bi-PIP

2024/1/25

Bi-PIP: Conjugates of a BD inhibitor (Bi) and PIP



- Some proteins have both HAT domain and bromodomain (BD).
- One acetyl mark causes acetylation of neighboring sites via BD-mediated recruitment of these proteins.



Bi-PIP

Figure 1. Strategy of targeted histone acetylation utilizing the bromodomain (BD)-mediated propagation of acetylation. (a) Structure of P300/CBP coactivator proteins. NRID, nuclear receptor interacting domain; TAZ1, transcriptional adaptor zinc finger 1; KIX, KID-interacting; BD, bromodomain; RING, really interesting new gene; PHD, plant homeodomain; HAT, histone acetyltransferase; ZZ, ZZ-type zinc finger; TAZ2, transcriptional adaptor zinc finger 2; IBiD, interferon-binding domain. (b) BD-mediated propagation of histone acetylation by P300/CBP. Existing acetyl lysine (yellow) is recognized by BD of P300/CBP, and de novo acetyl modification (green) is introduced by HAT domain. (c) Design of artificial epigenetic code of acetylation named “Bi-PIP” (left) and model of targeted histone acetylation by Bi-PIP (right). Bi mimics acetyl lysine to recruit P300/CBP through its BD.

This work

Localization to a specific DNA sequence of a BD inhibitor by “Bi-PIP”

→ Localization of a HAT-BD protein → Locus-specific histone acetylation

2024/1/25

Design of Bi-PIP

- Bi = one of the CBP30 (P300/CBP selective BD inhibitor) derivatives

- The target sequence of PIP

Bi-PIP1 → 5'-WWCWGCW-3' (8bp)

Bi-PIP2 → 5'-WWCCGCCW-3' (8bp)

(W = A or T)

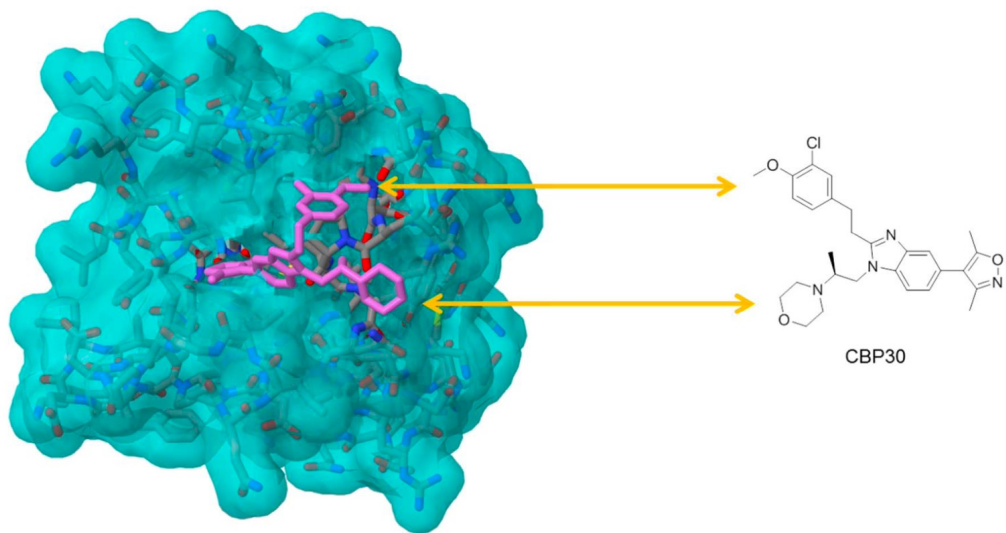
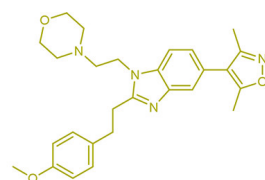
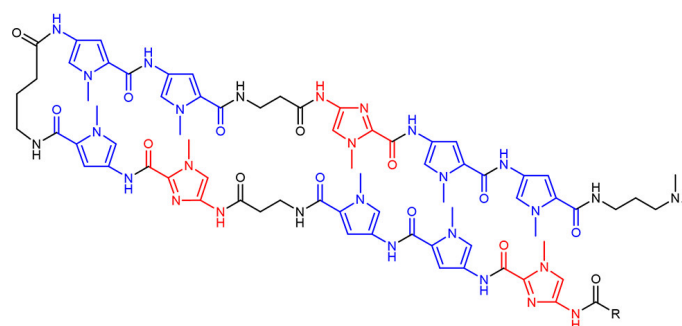
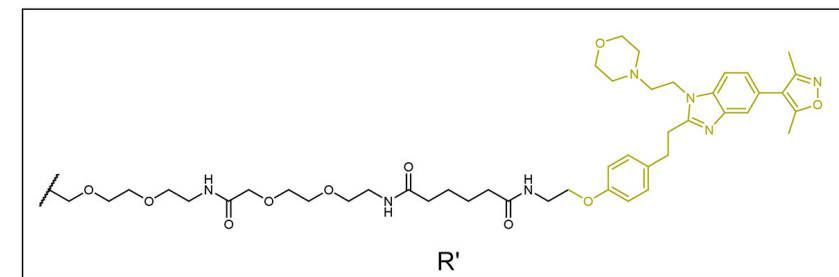


Fig.S1. Structural analysis of CBP30–CBP bromodomain complex.

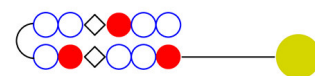
An X-ray crystal structure of P300 bromodomain bound by its inhibitor CBP30 (PDB ID: 5BT3) was analysed. The terminal aryl group and morpholine group are located outside of the bromodomain pocket. Arrows indicate the corresponding moieties.



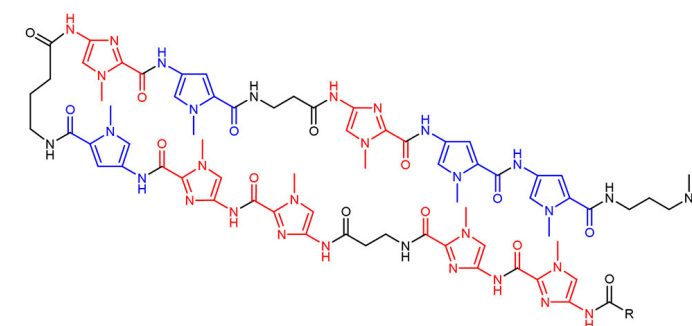
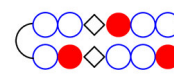
Bi (1)



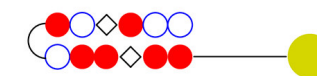
R = R' :
Bi-PIP1 (2)



R = Me :
PIP1 (3)



R = R' :
Bi-PIP2 (4)



R = Me :
PIP2 (5)

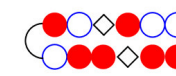


Figure 2. Chemical structures of Bi (1), Bi-PIP1 conjugate (2), PIP1 monomer (3), Bi-PIP2 conjugate (4), and PIP2 monomer (5).

Bi-PIPs promote histone acetylation on nucleosomes that have their target DNA sequences in vitro

Bi-PIP

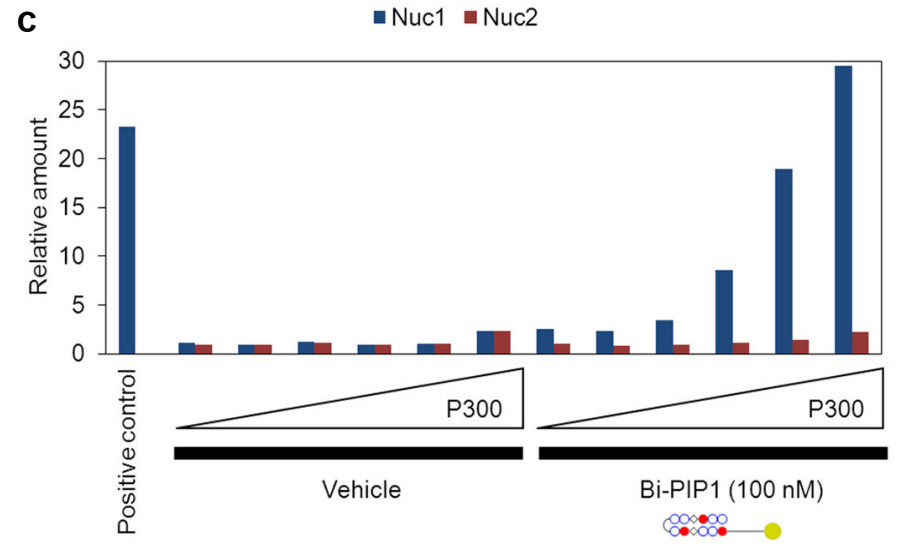
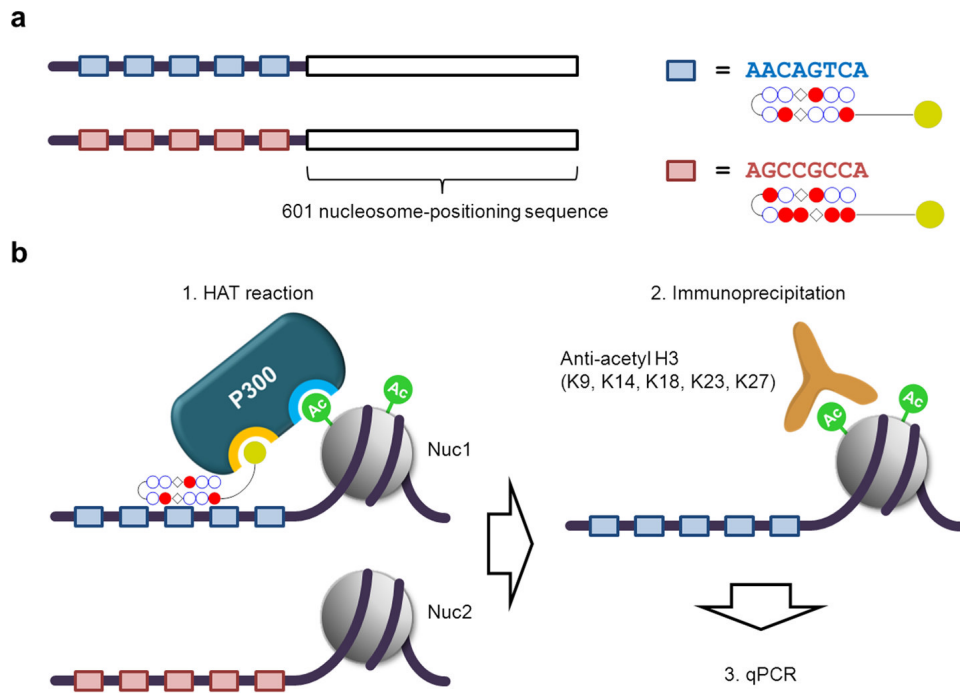
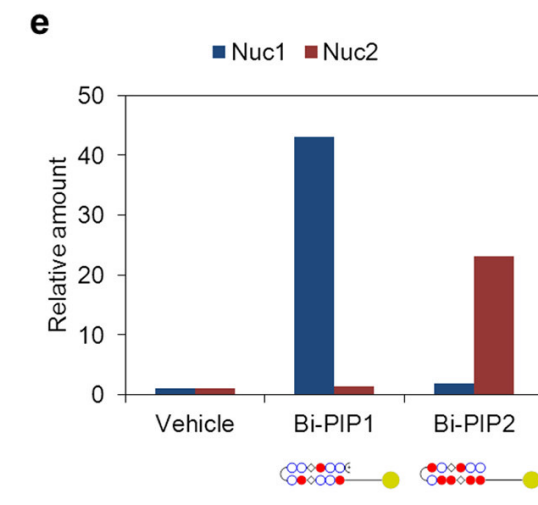
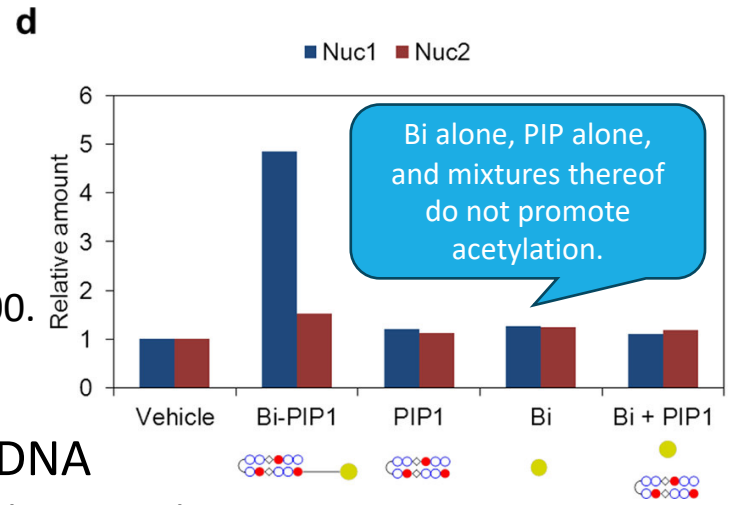
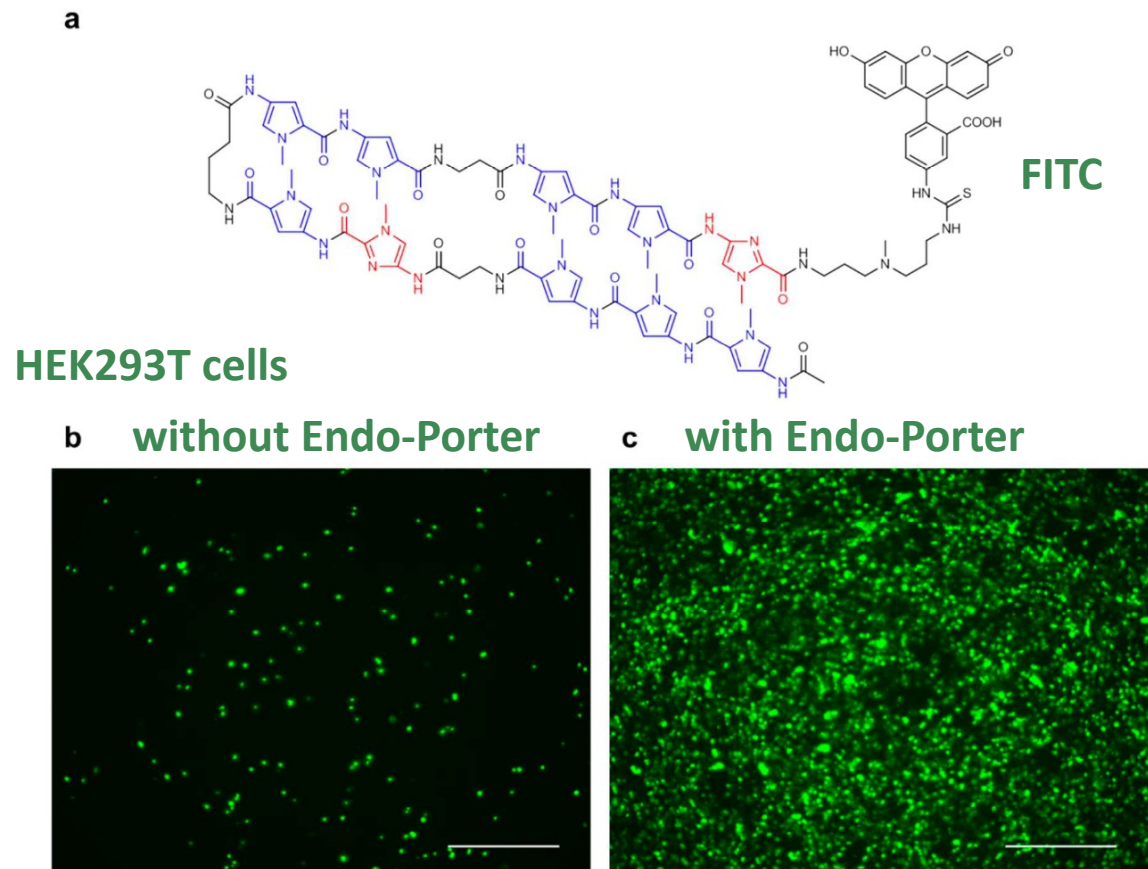


Figure 3. Bi-PIPs promote histone acetylation on nucleosomes that possess their target DNA sequences. (c) HAT reaction-in vitro ChIP-qPCR was performed with a series of P300 concentrations (0, 3, 10, 30, 100 nM) with or without 100 nM Bi-PIP1. Positive control represents a nucleosome with synthetic acetylated histone H3 (K4ac, K9ac, K14ac, K18ac, K23ac). (d) HAT reaction-in vitro ChIP-qPCR was performed with 10 nM of P300. Each compound was applied at a concentration of 100 nM. (e) HAT reaction-in vitro ChIP-qPCR was performed Bi-PIP1 (100 nM) or Bi-PIP2 (100 nM) with 10 nM of P300.

- ✓ 100 nM Bi-PIP1 induced intensive acetylation on its target Nuc1 but not on Nuc2.
- ✓ The level of acetylation was dependent on the concentration of P300.
- ✓ Acetylation was achieved by PIP binding to the target DNA sequence selectively and recruiting P300 by the BD-Bi interaction.



Cell permeability of PIPs



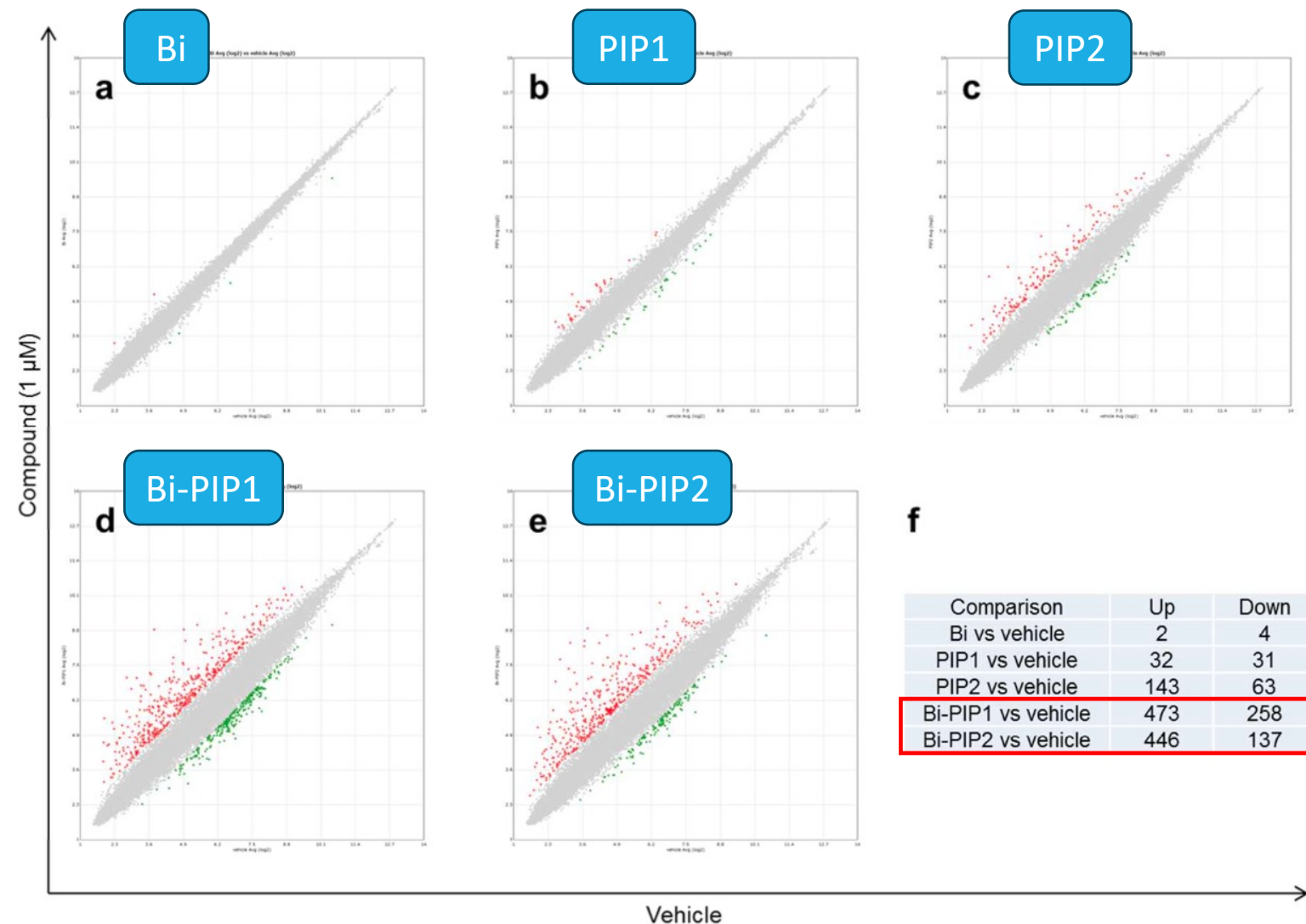
- The cell permeability of PIPs = vary depending on the chemical structures and cell lines
- ✓ Endo-Porter was used to ensure that all of the compounds enter the cells.

Fig.S9. PIP delivery with Endo-Porter

(a) Chemical structure of the FITC-labelled PIP used in the experiment. (b,c) HEK293T cells were treated with 0.9 μ M of the FITC-PIP alone (b) or 0.9 μ M of the FITC-PIP and Endo-Porter (4 μ M). Bars, 300 μ m.

Bi-PIP caused greater changes in gene expression

Bi-PIP



HEK293T cells

A transcriptome analysis of total RNA extracted from cells

✓ Bi-PIP1 and Bi-PIP2 gave greater transcriptome changes, mainly for activation.

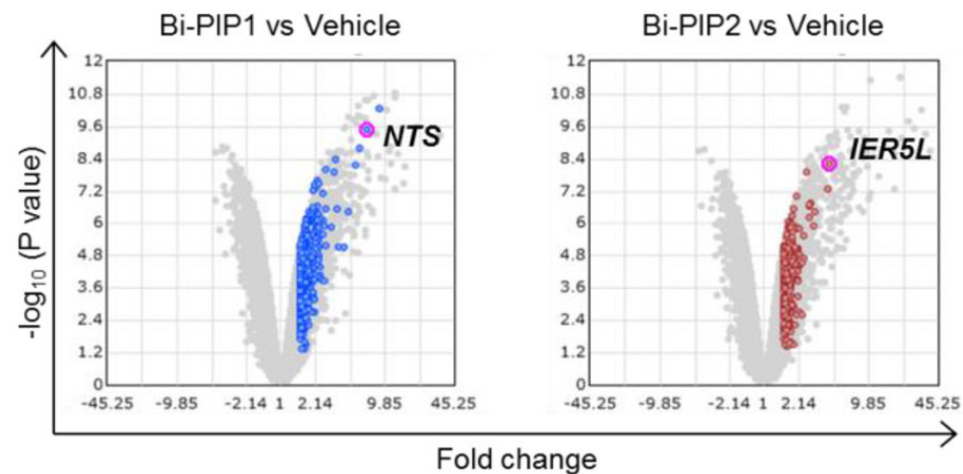
Fig.S10. Genome-wide gene expression change by each compound. (a–e) Scatter plots of cells treated with Bi (a), PIP1 (b), PIP2 (c), Bi-PIP1 (d), or Bi-PIP2 (e) versus vehicle-treated cell. Red and green dots represent transcripts which were up- or downregulated in each comparison. >2 or <-2 fold change and <0.05 P value were used as the criteria. (f) Summary of the number of differentially expressed genes.

After 15 hours of compound treatment, RNA was extracted.

2024/1/25

Bi-PIPs selectively activated gene expression in living cells

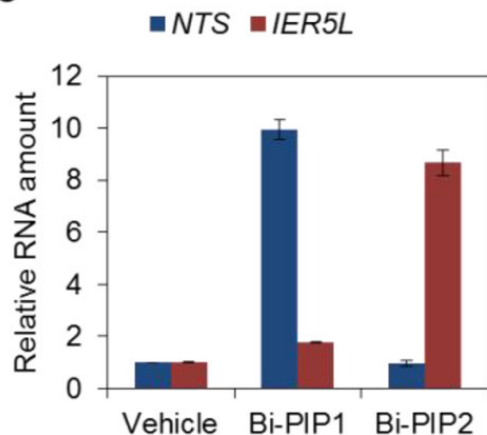
b



Uniquely activated transcripts by Bi-PIP and Bi-PIP2
→ NTS (neurotensin) and IER5L (immediate early response 5-like)

- NTS locus contains the binding sites for Bi-PIP1 but not for Bi-PIP2.
- IER5L locus contains the binding sites for Bi-PIP2 but not for Bi-PIP1.

c



d

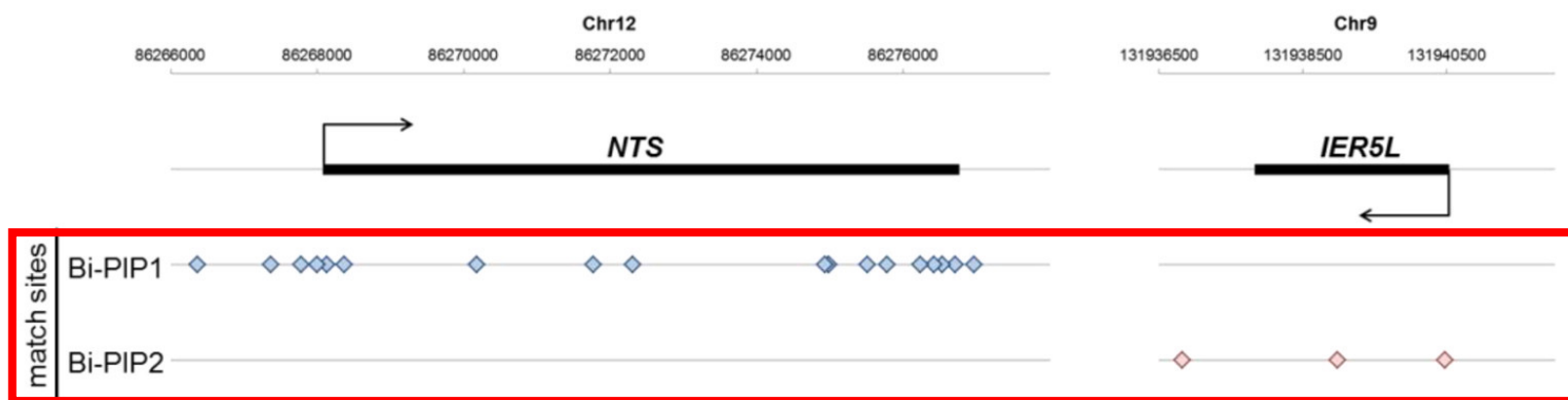


Figure 4. Bi-PIPs epigenetically activate selective gene expression inside living cells. (b) Volcano plots of transcriptome comparison of Bi-PIP1 vs vehicle (left) and Bi-PIP2 vs vehicle (right). Uniquely upregulated transcripts by individual Bi-PIP (>1.5 fold change) are indicated as colored dots. (c) Expression of *NTS* and *IER5L* was confirmed by RT-qPCR. Error bars represent standard deviation of data from two culture wells. (d) Genomic loci of *NTS* (top) and *IER5L* (bottom). Match sites for Bi-PIP1 (5'-WWCWGCW-3') and Bi-PIP2 (5'-WGCCGCCW-3') are indicated as blue and red diamonds, respectively.

2024/1/25

Acetylated loci by Bi-PIPs

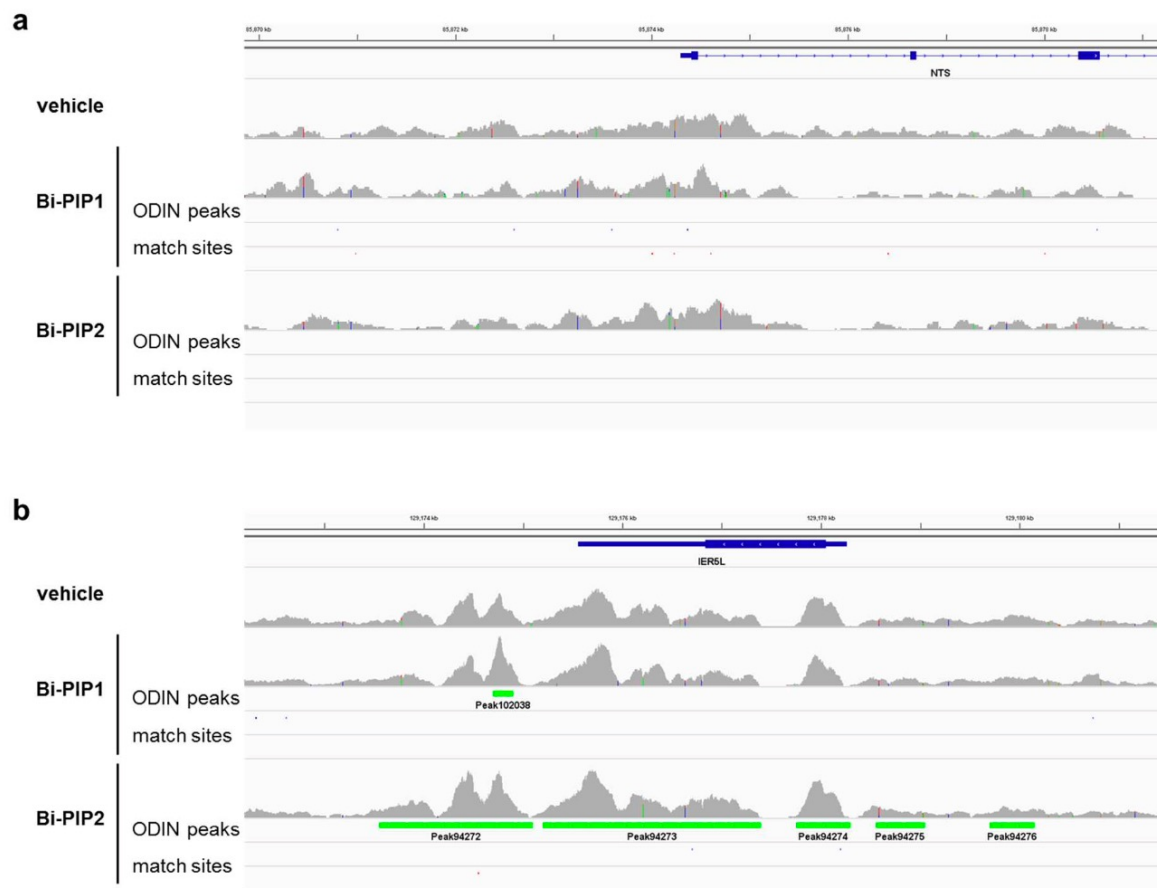


Fig.S12. ChIP-seq analysis on activated gene loci. anti-acetylated H3 Mapped reads in ChIP-seq, differential peaks significantly increased in Bi-PIP vs vehicle detected by ODIN, and match sites of Bi-PIPs at *NTS* locus (a) and *IER5L* locus (b) are shown.

- ✓ The acetylation at NTS locus slightly increased by Bi-PIP1.
- ✓ The acetylation at IER5L locus increased by Bi-PIP2.

△ Acetylated loci by Bi-PIP
= its target sequences + the **other** possible binding sites

Summary of Bi-PIP & Challenges

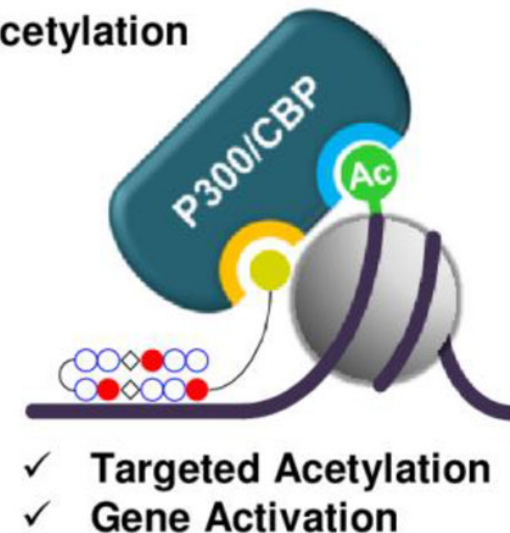
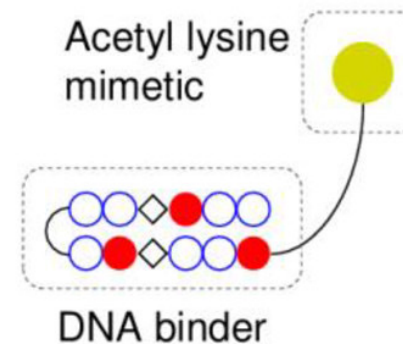
Summary

- ✓ Bi-PIP recruited P300/CBP to selective DNA sequences.
- ✓ Bi-PIP promoted the sequence-selective histone acetylation and transcriptional activation in living cells without gene transfection.

Challenges

- Need to improve the sequence-selective ability
- Endogenous enzyme-dependent

Bi-PIP: Artificial Epigenetic Code of Acetylation



- Introduction
- KR12 (DNA alkylating agent with PIP)
- Bi-PIP (Brd inhibitor with PIP)
- **PIP-HoGu (Integration of PIP and cooperative systems)**
- ePIP-HoGu (PIP-HoGu with epigenetic modulator)
- Summary & Discussion

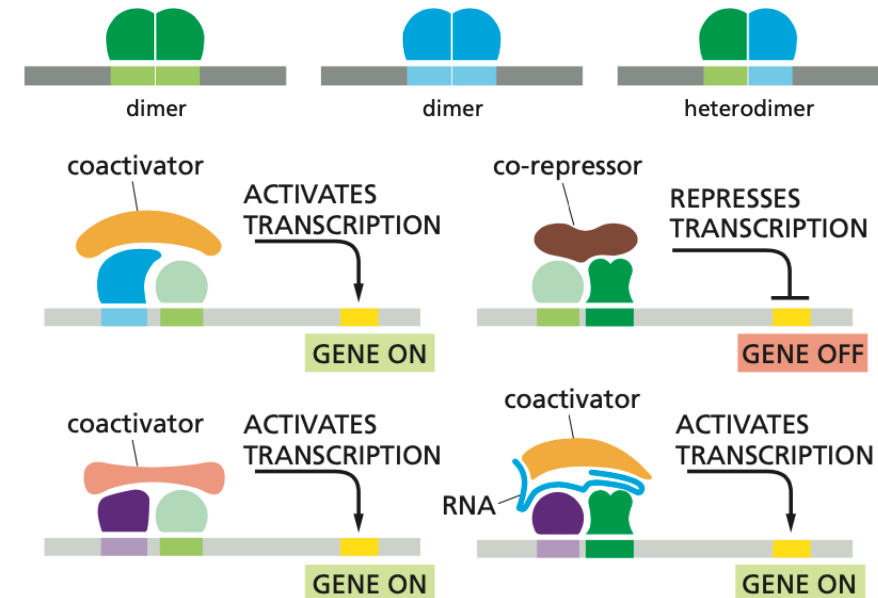
TFs often act as homo/heterodimers

Current challenges

- The short recognition sequence of PIP leads high off-target rates.
- The extension of PIP length significantly reduces its cell permeability.
- Single PIP cannot block interactions between TF **pairs** and DNA.

✘ Transcription factors (TFs) often act as **homo/heterodimers**

→ **high binding affinity** and **extended recognition sequences**



Design for mimicking cooperative TF-pair systems

PIP-HoGu

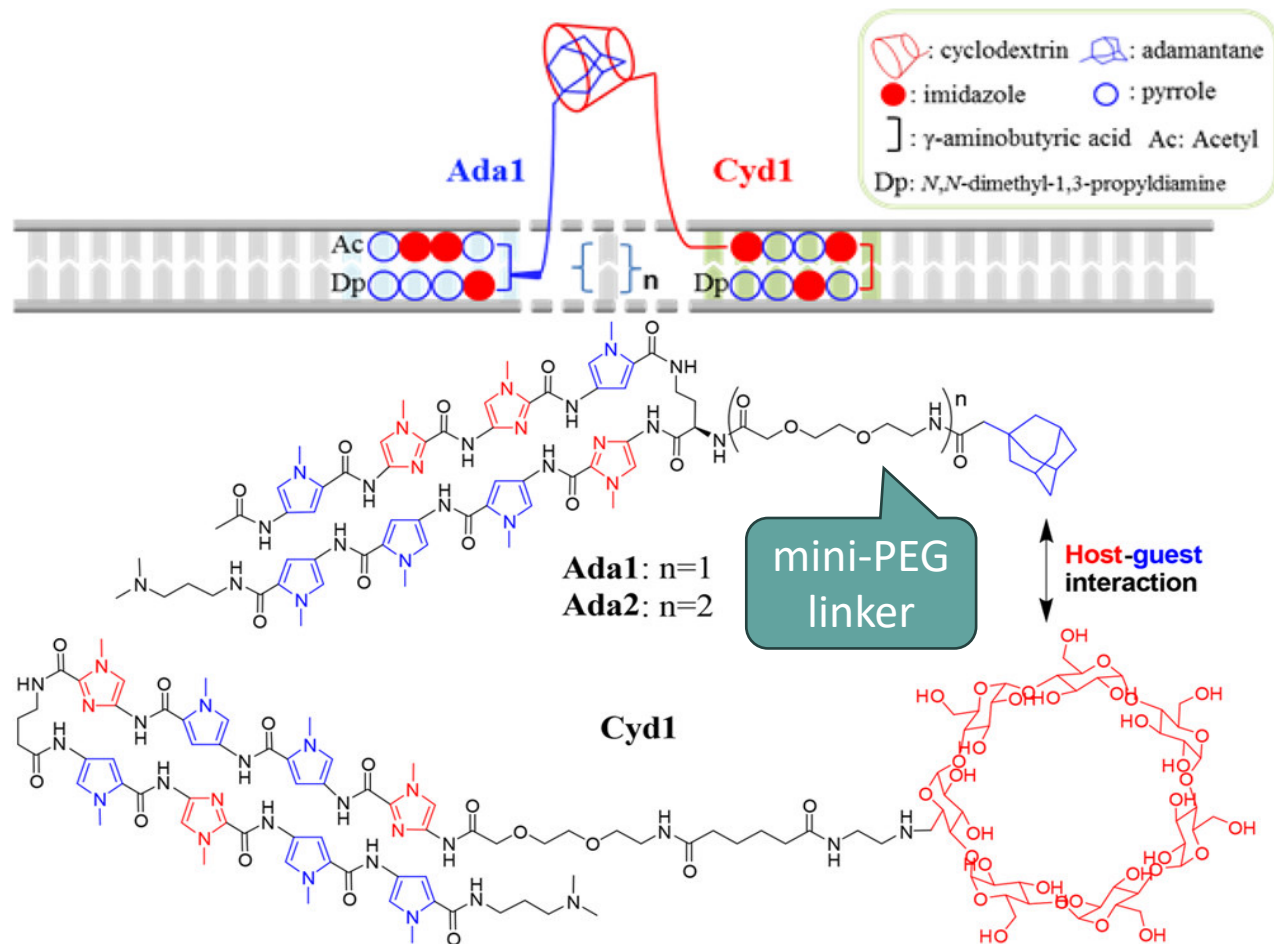


Figure 1. Overview of cooperative interactions of a TF pair targeting a sequence associated with two components of Pip-HoGu assembly, Ada1 and Cyd1. n = gap distance. (Bottom) Chemical structures of Ada1, Ada2, and Cyd1.

Strategy

- Integration of PIPs with a cooperative system
→ Noncovalent cooperative system
(nucleic acid analogues, metal ion-ligand, **host-guest systems (ex. cyclodextrin(Cyd)-adamantane(Ada))**)

This work

1. Design PIP-HoGu (PIPs conjugated to a host-guest Cyd-Ada scaffold)
2. Evaluate PIP-HoGu in vitro using the DNA binding sequences of the Tax/CREB heterodimer
3. Experiment in cells

2024/1/25

0-5 bp gap distances displayed cooperative binding.

A

Gap distance (n)	Positive binding mode		Negative binding mode	
	ODNs	Diagram	ODNs	Diagram
-1	1'P	5'-AAACTTAGGCTGACGTATATAT-3'	1'N	5'-AAACTTGACG-TAGGCTATATAT-3'
0	0P	5'-AAACTTAGGCTTGACGTATATA-3'	0N	5'-AAACTTGACGTTAGGCTATATA-3'
1	1P	5'-AACTTAGGCTATGACGTATATA-3'	1N	5'-AACTTGACGTATAGGCTATATA-3'
2	2P	5'-AACTTAGGCTAATGACGTATAT-3'	2N	5'-AACTTGACGTAATAGGCTATAT-3'
3	3P	5'-AACTTAGGCTAAATGACGTATAT-3'	3N	5'-AACTTGACGTAATAGGCTATAT-3'
4	4P	5'-AACTTAGGCTATTATGACGTATAT-3'	4N	5'-AACTTGACGTATTATAGGCTATAT-3'
5	5P	5'-AATTAGGCTATTAATGACGTATAT-3'	5N	5'-AATTGACGTAATTAATAGGCTATAT-3'
6	6P	5'-AATTAGGCTAATTAATGACGTATA-3'	6N	5'-AATTGACGTAATTAATAGGCTATA-3'

impossible for Ada to interact with Cyd

Thermal stabilization assay

(ΔT = difference in melting temperature)

- ✓ improved thermal stability by the cooperative interaction of the Cyd-Ada complexes
- ✓ gap 0-5 bp → cooperative binding function
- ✓ 2 bp gap → the highest level of cooperation ($\Delta\Delta T_m = 7.2$ °C)

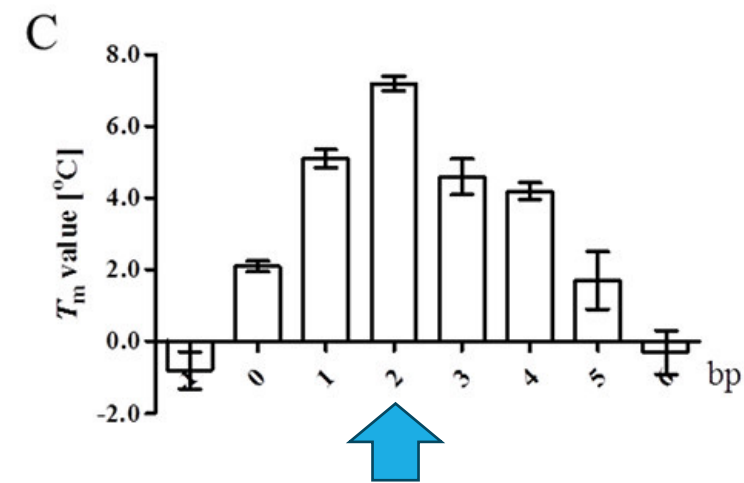
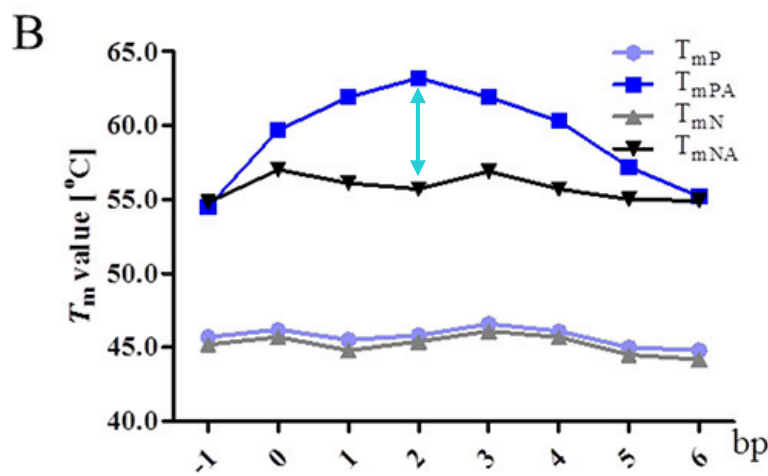


Figure 2. T_m assay illustrating the cooperativity of Pip-HoGu. (A) The DNA oligomers (ODNs) used in the T_m assay, including positive (ODN1'P-ODN6P) and negative (ODN1'N-ODN6N) binding sequences. The gap distance (green) is the number of bp between the binding sites of Ada1 (blue) and Cyd1 (red). The chart only shows the forward DNA strand. (B) T_m profiles of positive ODNs (T_{mP}, light blue), negative ODNs (T_{mN}, gray), positive ODNs/Ada1-Cyd1 (T_{mPA}, blue), and negative ODNs/Ada1-Cyd1 (T_{mNA}, black). (C) $\Delta\Delta T_m$ profiles of cooperativity of Ada1-Cyd1 assemblies. $\Delta T_m = T_m(\text{ODNs/PIPs}) - T_m(\text{ODNs})$; $\Delta\Delta T_m = \Delta T_{mP} - \Delta T_{mN}$. Error bars indicate the standard deviation of three replicates.

PIP-HoGu has high sequence-selectivity.

PIP-HoGu

Table S2. Results of T_m assay of mismatch sequence

ODNs	T_m [°C]	T_{mPA} [°C]	ΔT_{mA} [°C] ^a	$\Delta\Delta T_m$ [°C]
ODN2P	45.8	63.2	17.4	8.4
ODN2PM	43.9	52.9	9.0	

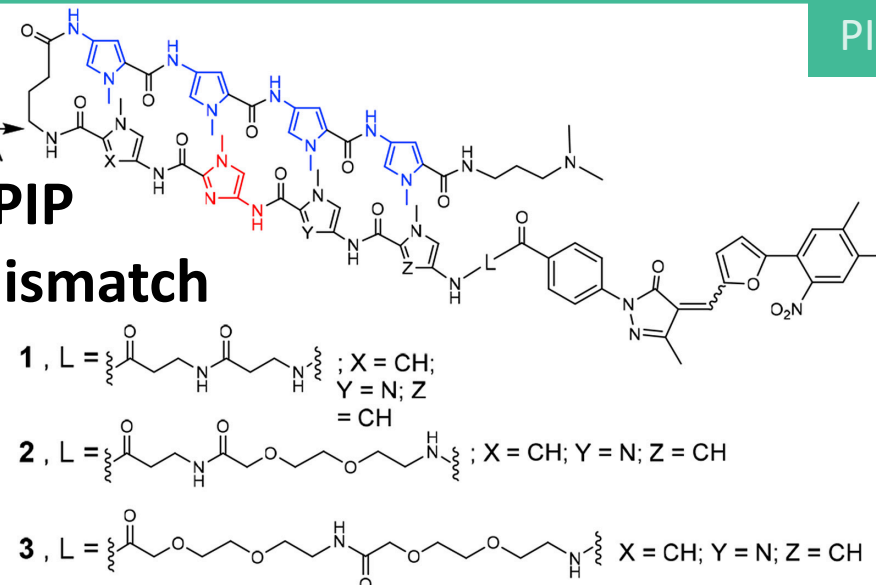
ODN2P: 5'-AACTTAGGCTAATGACGTATAT-3'

ODN2PM: 5'-AACTTAGGCTAATGATGTATAT-3'

- 1-bp mismatch T_m assay
- ✓ PIP-HoGu exhibited high sequence-selectivity.

cf)

Single PIP 3-bp mismatch



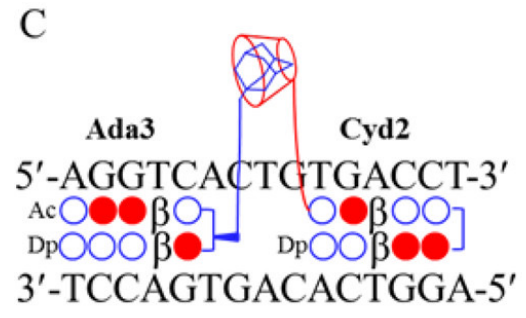
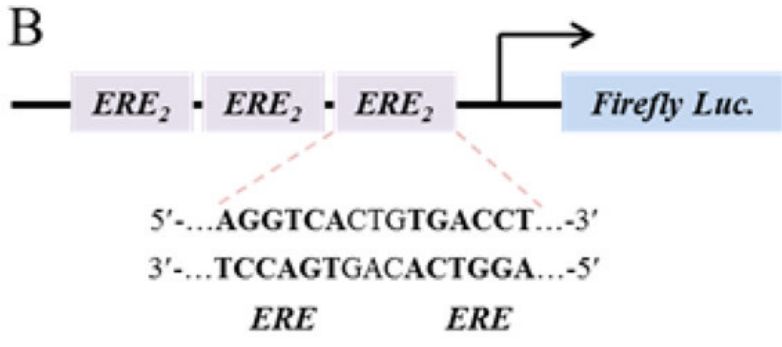
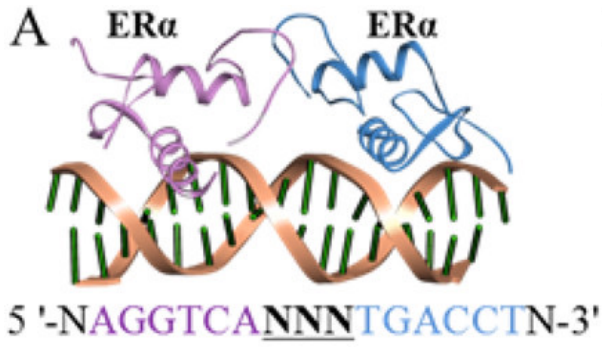
Conjugates	Match sequence	Mismatch sequence				
	ODN1: 5'-ACTTATTCATATAGA-3'	ODN3: 5'-ACTTATCCACTATAGA-3'				
	ODN2: 3'-TGAATAAGGTATATCT-5'	ODN4: 3'-TGAATAGGTGATATCT-5'				
	$T_m = 32.5$ °C (± 0.1)	$T_m = 34.3$ °C (± 0.1)				
	T_m /°C	ΔT_m /°C ^a	$\Delta\Delta T_m$ /°C	T_m /°C	ΔT_m /°C	$\Delta\Delta T_m$ /°C ^b
1	49.4 (± 0.1)	16.9	-	45.3 (± 0.1)	11.0	5.9
2	50.6 (± 0.1)	18.1	-	45.8 (± 0.1)	11.5	6.6
3	50.9 (± 0.1)	18.4	-	46.5 (± 0.1)	12.2	6.2

2024/1/25

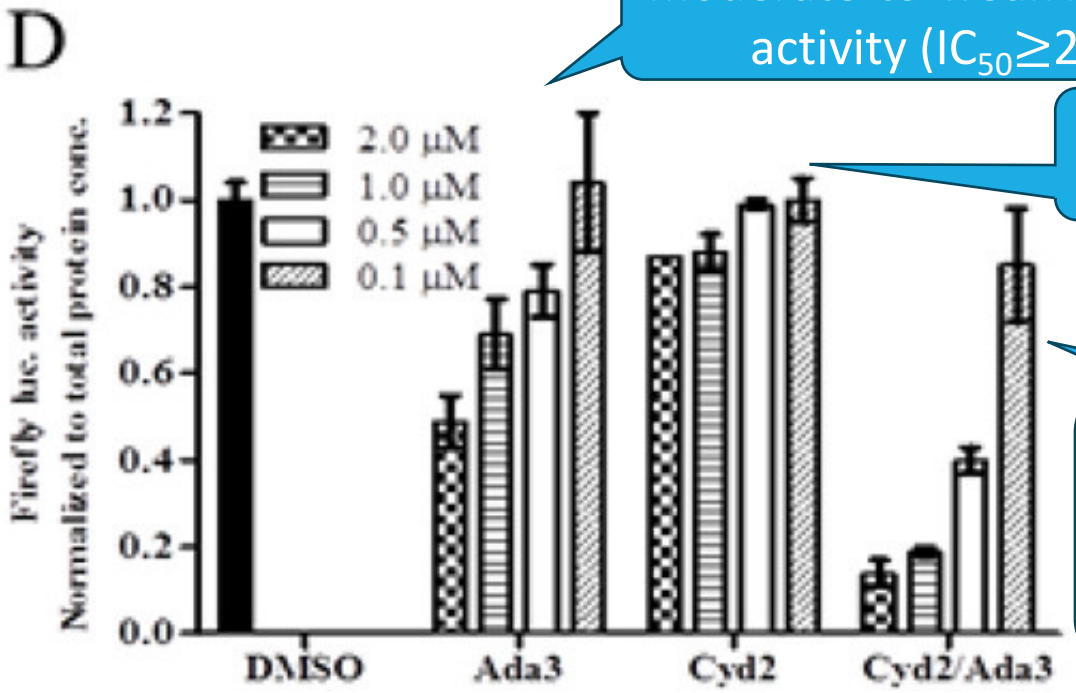
PIP-HoGu inhibited natural TF-pair binding in cells.

PIP-HoGu

Figure 5. Cell-based assay of Pip-HoGu. (A) Crystal structure of E α homodimer and DNA sequence. (B) Schematic diagram of ERE-driven luciferase in T47D-KBluc cells. (C) The structural design of Ada3 and Cyd2 targeting ERE sites (Figure S8). (D) Luciferase activity assay after normalization to the total protein concentration.



※ERE (estrogen response element)= specific target motif of the estrogen receptor α (ER α) homodimer



moderate-to-weak inhibitory activity ($IC_{50} \geq 2 \mu M$)

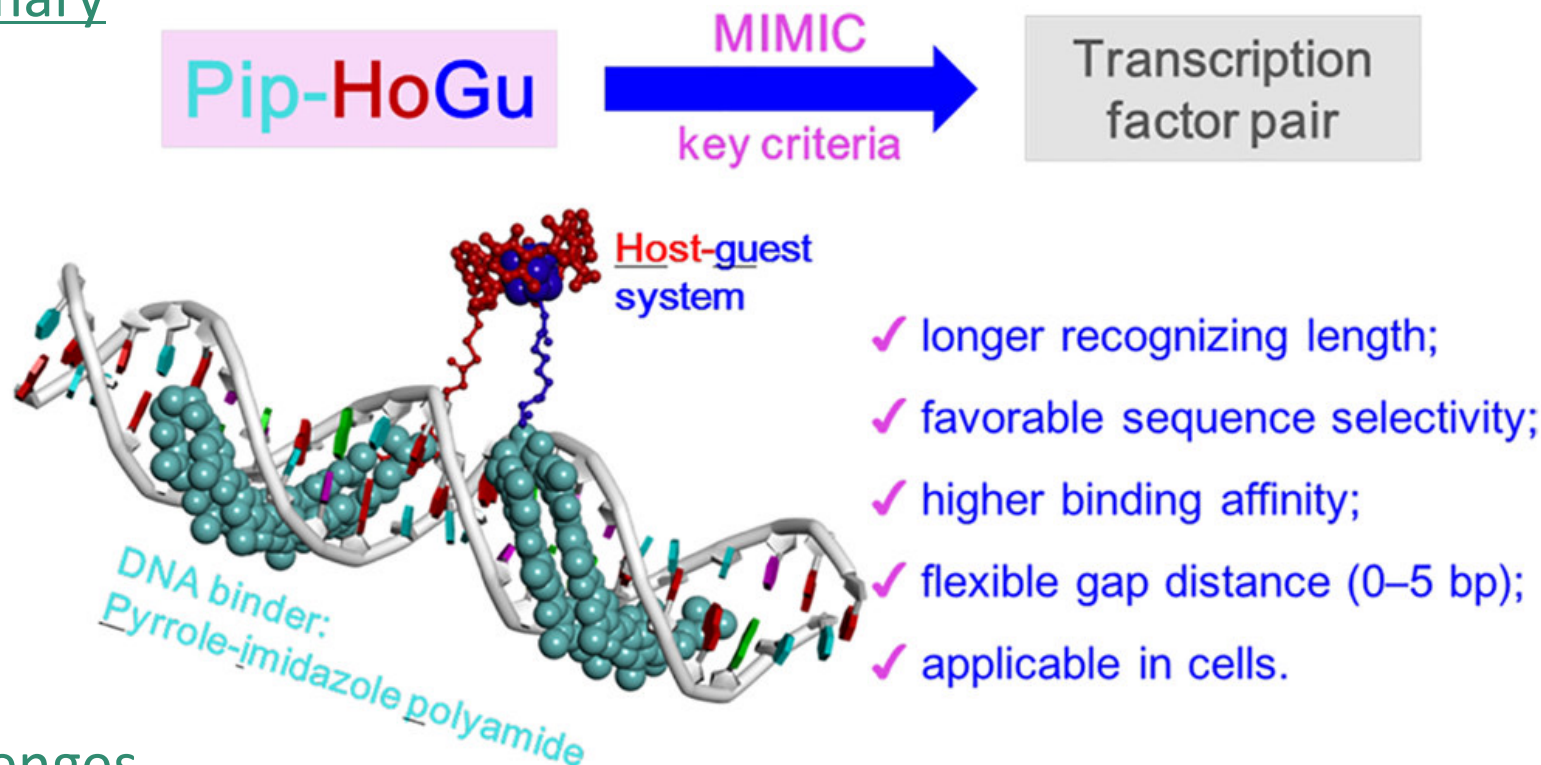
very weak activity (<20% inhibition)

4-5-fold enhancement of the inhibitory effect

- cell-based assay
- In ER α -positive, 17 β -estradiol-stimulated T47D-KBluc cells (highly express luciferase after binding three ER α TF pairs)
- Ada3 only vs. Cyd2 only vs. Ada3-Cyd2** \rightarrow luciferase activity was measured
- ✓ PIP-HoGu potently inhibited natural TF pairs in cell.

Summary of PIP-HoGu & Challenges

Summary



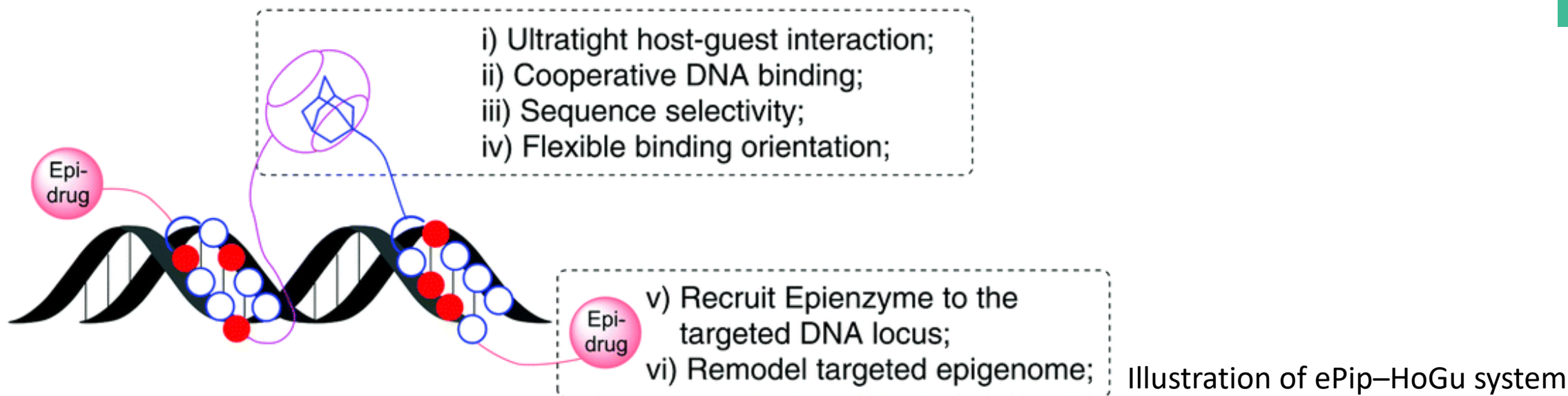
Challenges

- Limitation of gap distance (~5 bp)
- Optimization of the host-guest moiety

- Introduction
- KR12 (DNA alkylating agent with PIP)
- Bi-PIP (Brd inhibitor with PIP)
- PIP-HoGu (Integration of PIP and cooperative systems)
- **ePIP-HoGu (PIP-HoGu with epigenetic modulator)**
- Summary & Discussion

A synthetic mimic capable of cooperative DNA binding and epigenetic modulation

ePIP-HoGu



Motivation

TFs → cooperative DNA binding & **transcriptional modulation**

Need to create a synthetic mimic that can perform both **cooperative DNA binding** and **epigenetic modulation**

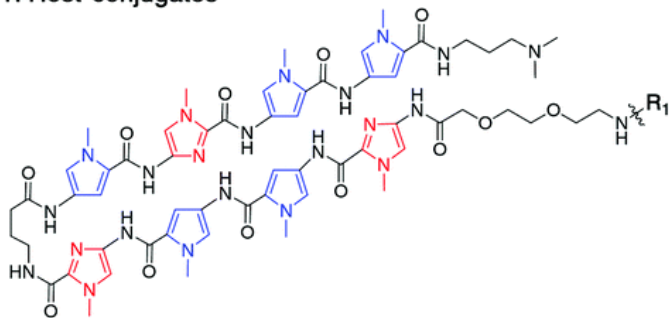
Strategy

The installation of an epigenetic modulator (epi-drug) to PIP-HoGu

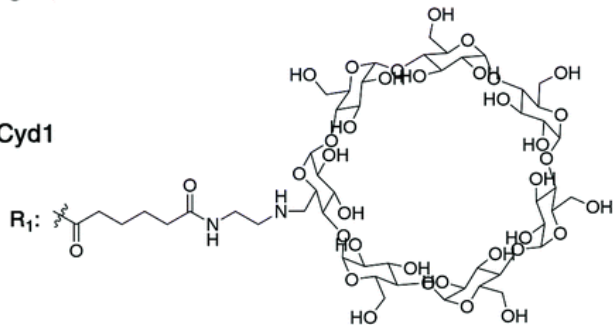
2024/1/25

Upgraded the cooperation domain in PIP–HoGu system

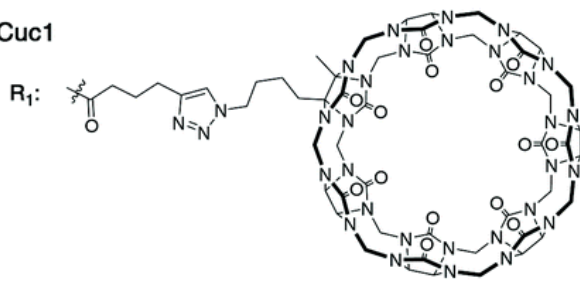
1. Host conjugates



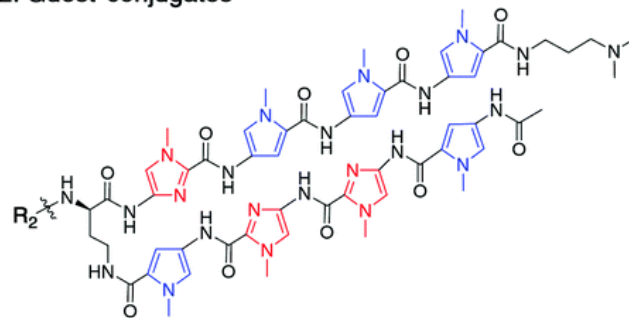
Cyd1



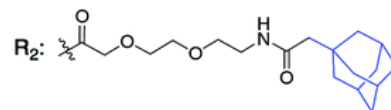
Cuc1



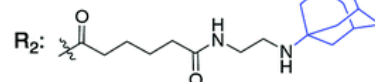
2. Guest conjugates



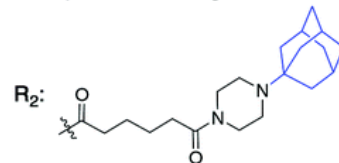
Ada1: flexible linker



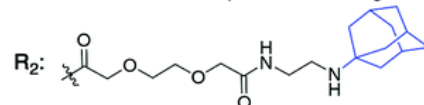
Ada3: positive charge at NH⁺



Ada5: positive charge at NH⁺



Ada6: flexible linker; positive charge at NH⁺



Improvement of PIP-HoGu replacing Cyd with CB7

*CB7 = cucurbit[7]uril

- CB7-PIP (Cuc1)
- Ada1-6 (Linker length, type, and positive charge are different)

Fig. 2 Chemical structures of host conjugates CB7–PIP and Cyd–PIP (A), and guest conjugates Ada–PIP (B).

Cuc1 exhibited higher affinity than Cyd1

Table S3. T_m assay of Cyd1- and Cuc1-guest conjugates with ODNs containing 2 bp spacing

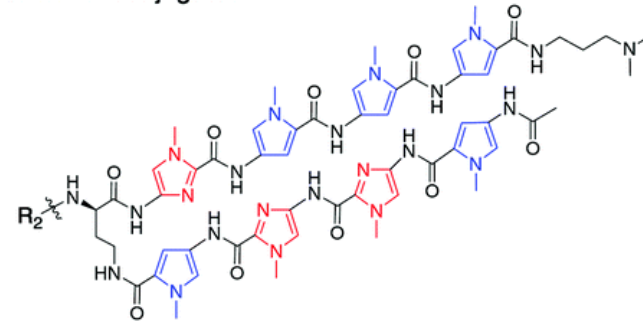
Host \ Guest	Ada1	Ada3	Ada5	Ada6
Cyd1	63.2 ± 0.3	63.5 ± 0.2	63.1 ± 0.3	62.9 ± 0.4
Cuc1	64.5 ± 0.2	65.6 ± 0.1	63.6 ± 0.4	64.7 ± 0.1
ΔT_m	1.3 ± 0.5	2.2 ± 0.3	0.6 ± 0.7	1.8 ± 0.5

$\Delta T_m = T_m(\text{ODNs/Cuc1/Ada-PIP}) - T_m(\text{ODNs/Cyd1/Ada-PIP})$. ODNs (2P) forward strand is 5'-AACTTAGGCTAATGACGTATAT-3'. Error bars are ranging from 0.1–0.7 °C indicating standard deviation of three replicates.

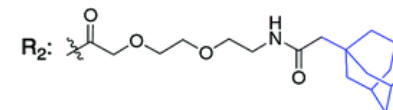
Thermal stabilization assay

- ✓ Cuc1 exhibited higher thermal stability than Cyd1
- ✓ Ada3 (with an ethyldiamino residue and alkyl chain) showed the most prominent stabilization

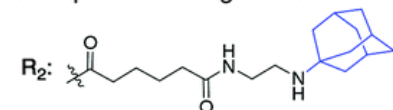
2. Guest conjugates



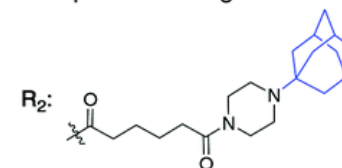
Ada1: flexible linker



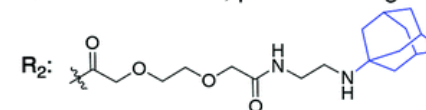
Ada3: positive charge at NH⁺



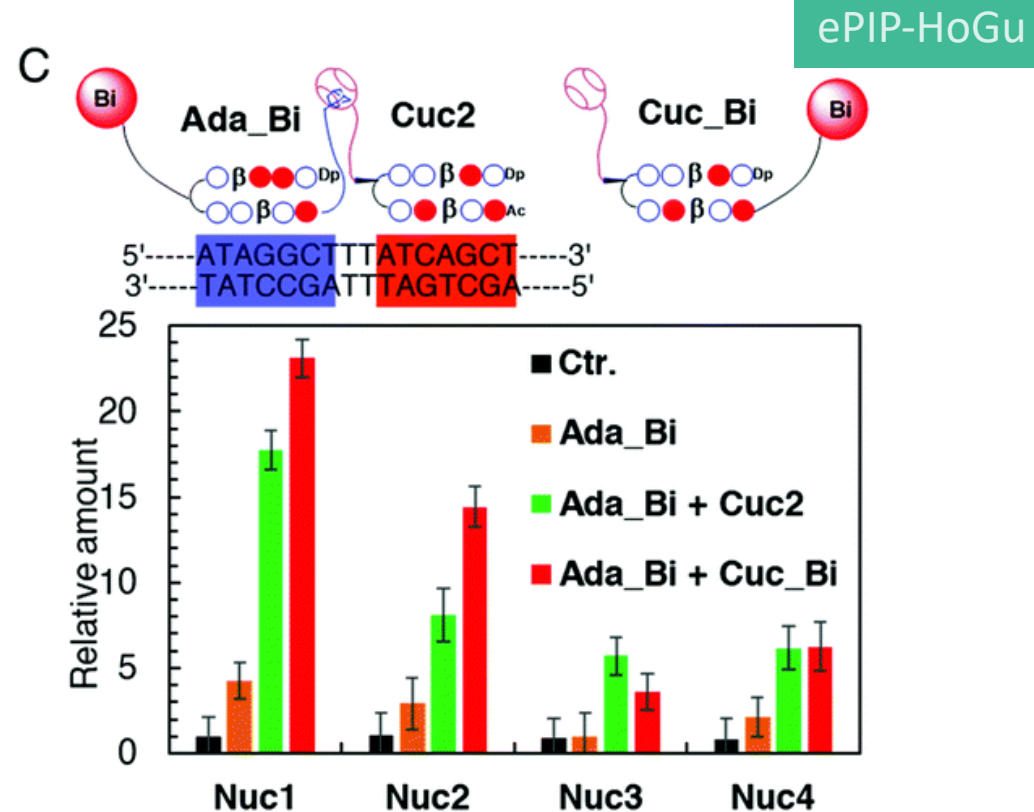
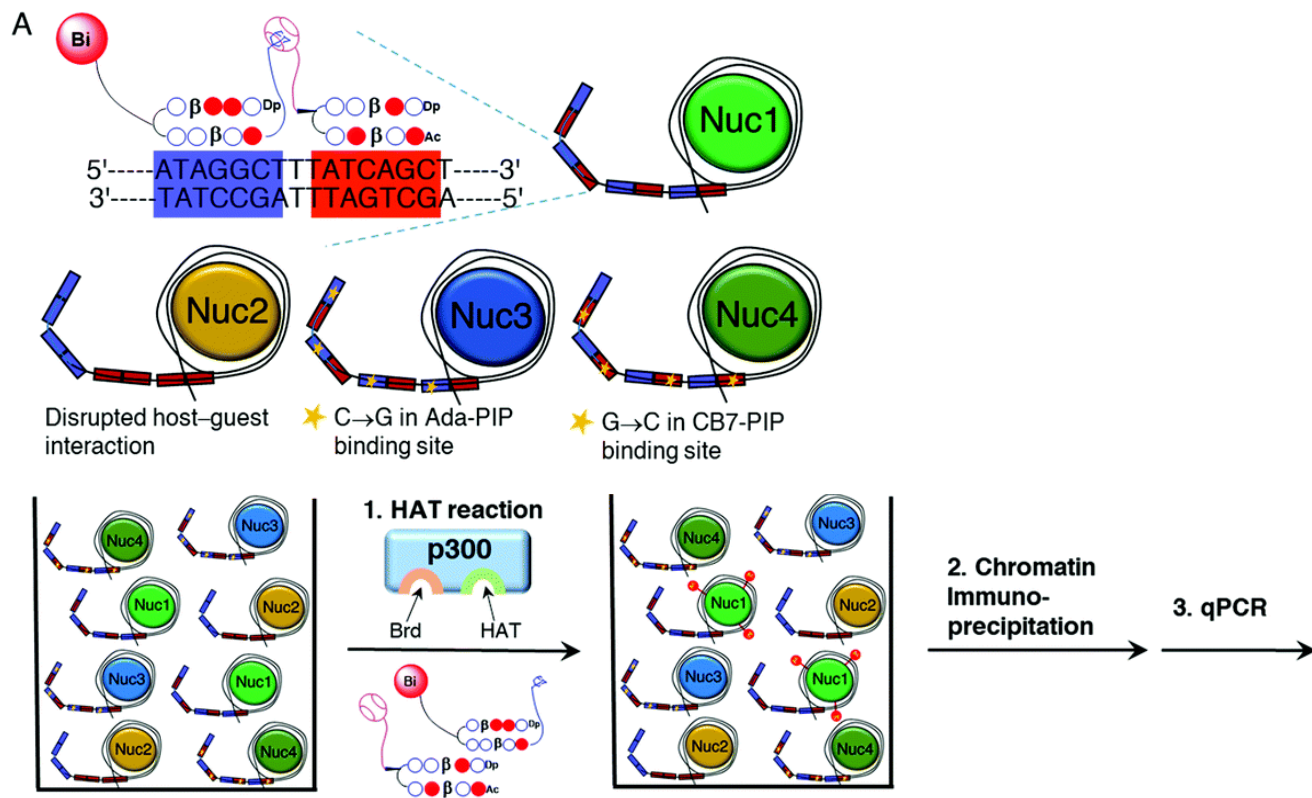
Ada5: positive charge at NH⁺



Ada6: flexible linker; positive charge at NH⁺



ePIP-HoGu recruited functional enzymes sequence-selectively.



- ✓ Co-treatment of **Ada_Bi1** and **Cuc2** hugely increased the acetylation level in Nuc1 (nearly 20-fold)
- ✓ Co-treatment of **Ada_Bi1** and **Cuc_Bi1** further enhanced the acetylation level in Nuc1 (23.5-fold)

Fig. 4 ePIP-HoGu synergistically recruits an epigenetic modifier to the target DNA repeat locus. (A) Schematic illustration of four kinds of nucleosomes with different DNA templates. Nuc1 contains four-matched repeat sequence of PIP-HoGu binding. Nuc2 has two homodimeric binding sites of Ada-PIP and CB7-PIP separately, which cannot form a host-guest interaction (Nuc2 has potential synergic binding partially between site 2 and 3, because of the short distance between them). One-mismatch bp localizes in the binding site of Ada-PIP for Nuc3 and CB7-PIP for Nuc4. (B) The workflow of the *in vitro* HAT-ChIP-qPCR assay. (C) Results of the *in vitro* HAT-ChIP-qPCR assay. Compound treatment in three groups compared with control (DMSO), i.e., Ada_Bi1, Ada_Bi1 + Cuc2, and Ada_Bi1 + Cuc_Bi1.

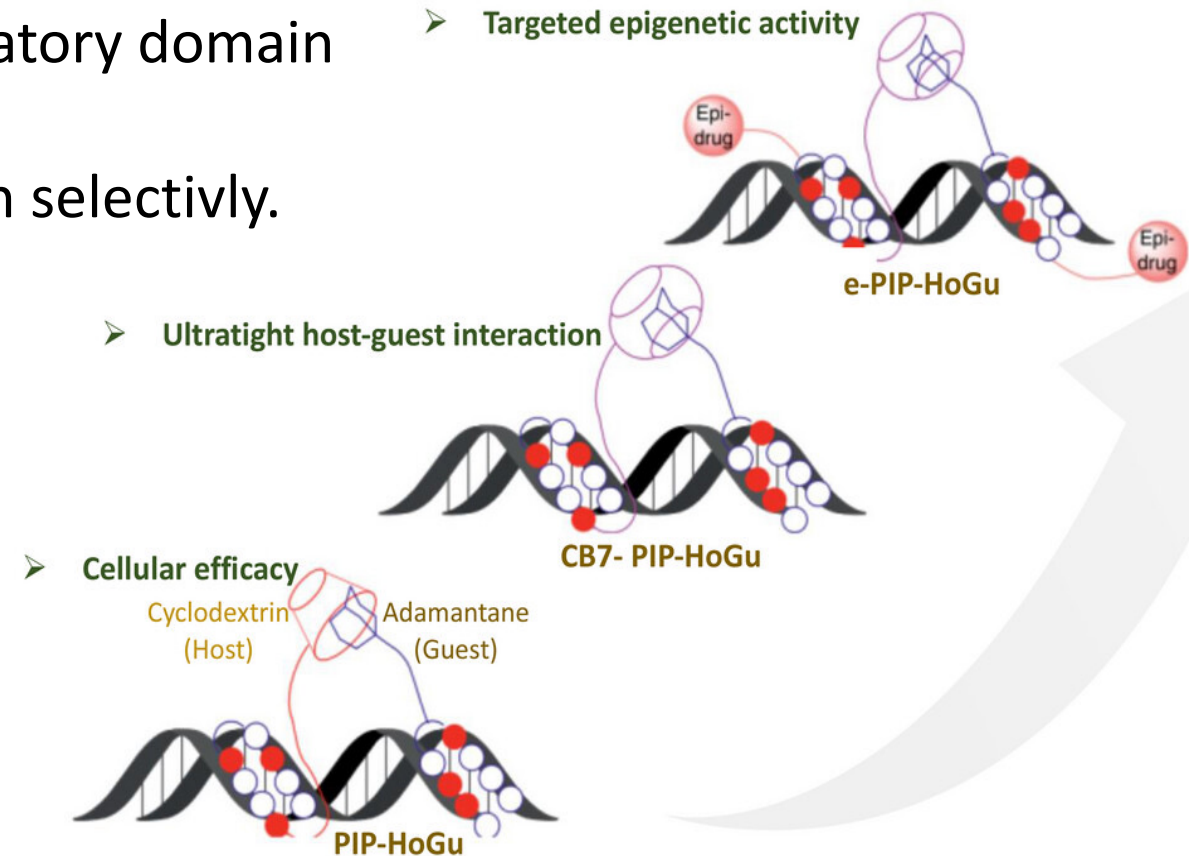
Summary of ePIP-HoGu & Challenges

Summary

- ✓ ePIP-HoGu contain a DNA binding domain, an interaction domain, and a gene regulatory domain like natural TF pairs.
- ✓ ePIP-HoGu promoted histone acetylation selectively.

Challenges

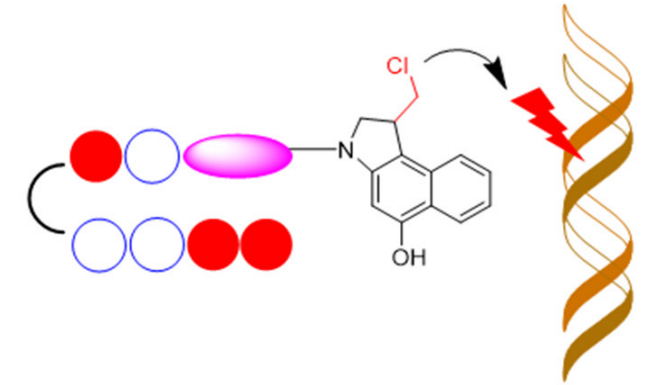
- Endogenous enzyme-dependent
- Cell-based assay
- Specific gene activation



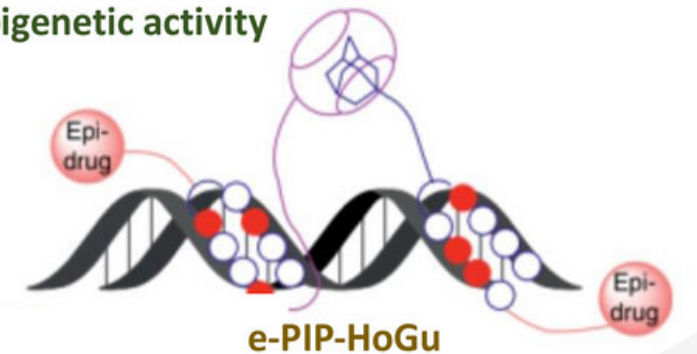
- Introduction
- KR12 (DNA alkylating agent with PIP)
- Bi-PIP (Brd inhibitor with PIP)
- PIP-HoGu (Integration of PIP and cooperative systems)
- ePIP-HoGu (PIP-HoGu with epigenetic modulator)
- **Summary & Discussion**

Summary

- ✓ PIPs can inhibit binding of transcription factors.
- ✓ Conjugating PIPs to DNA alkylating agents enhanced the effectiveness of the alkylating agent.
- ✓ Conjugating PIPs to epigenetic modulators enabled genomic loci-selective histone modifications.
- ✓ Conjugating PIPs to a cooperative binding system improved DNA sequence selectivity and binding affinity.



Targeted epigenetic activity



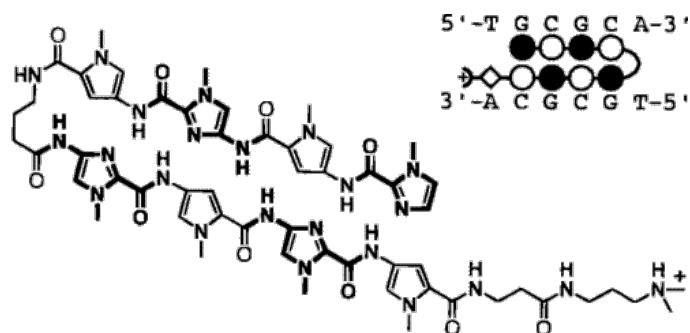
- ✓ PIPs have the potential to serve as **small molecule-based designer drugs in targeted transcription therapy.**
 - ◆ Cell permeability → PIP-HoGu
 - ◆ Conjugation with small molecule drugs (e.g., DNA alkylating agents)

- ✓ PIPs are programmable and can be applied to personalized precision medicine.
 - ◆ Need for optimization in each case

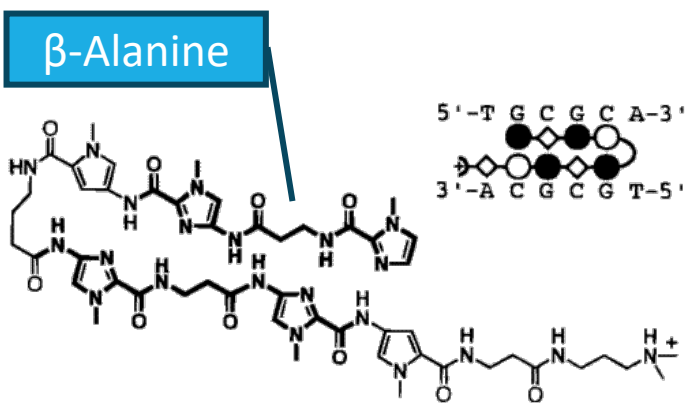
Thank you for your kind attention!

Appendix

β-Alanine can improve affinity and relax torsional rigidity



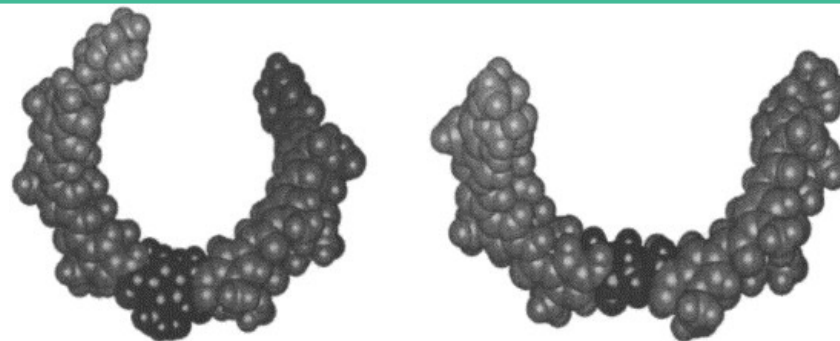
(11) ImPyImPy-γ-ImPyImPy-β-Dp $K_a = 3.7 (\pm 0.9) \times 10^7 \text{ M}^{-1}$



(12) Im-β-ImPy-γ-Im-β-ImPy-β-Dp $K_a = 3.7 (\pm 1.5) \times 10^9 \text{ M}^{-1}$

100-fold
increase
in affinity

Appendix (KR12)



✓ Relaxing torsional rigidity

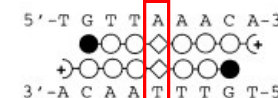
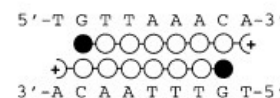


Table 3. Pairing code β-alanine (β), Py/Py and Im/Im pairs.^a

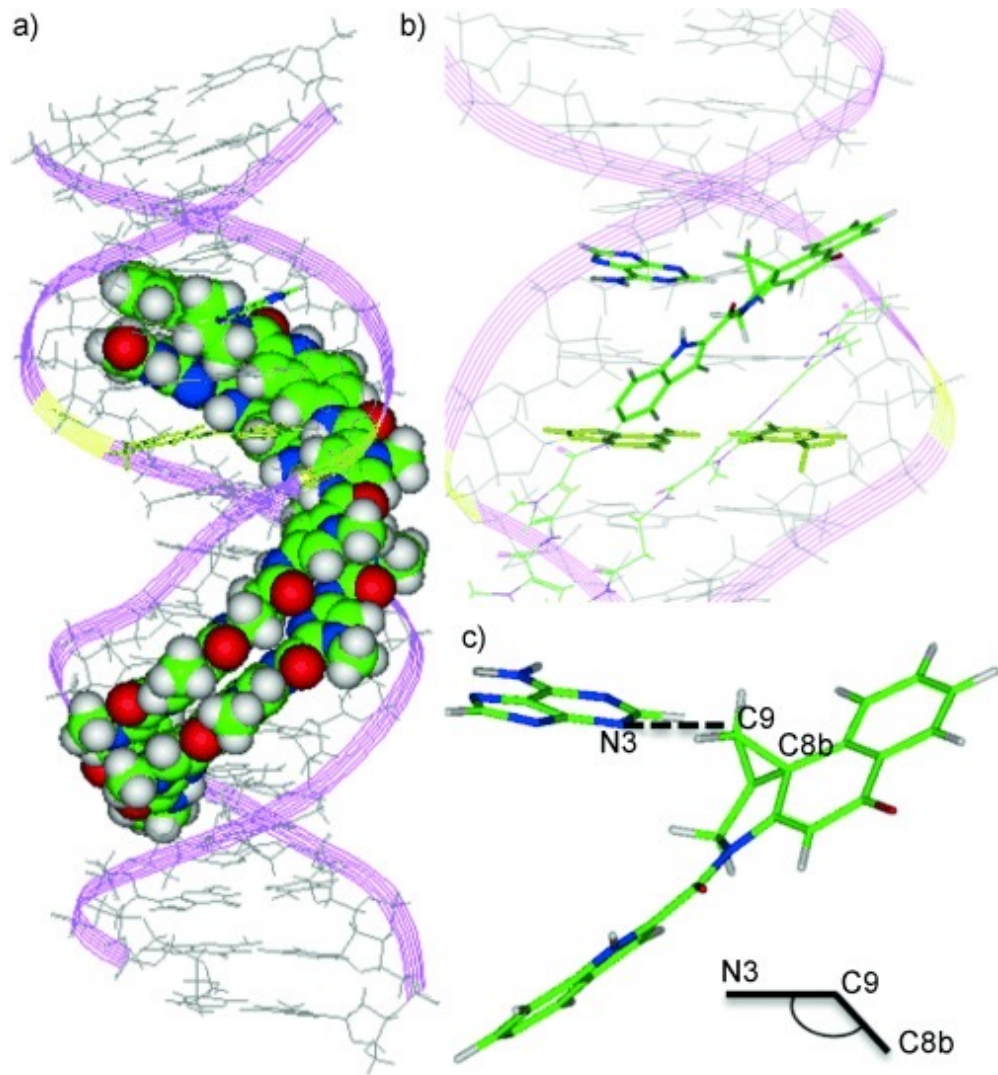
Pair	G•C	C•G	T•A	A•T
Im/β	+	–	–	–
β/Im	–	+	–	–
Py/β	–	–	+	+
β/Py	–	–	+	+
β/β	–	–	+	+
Py/Py	–	–	+	+
Im/Im	–	–	–	–

^aFavored (+), disfavored (–).

- PIP owning over **four continuous rings** shows high torsional rigidity.
- β-alanine linker = replacement for the Py moiety

Role of indole moiety in KR12

Appendix (KR12)



d)

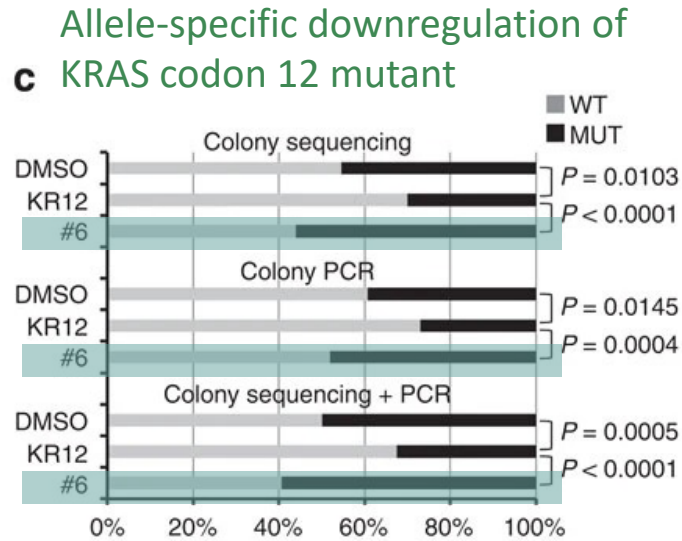
Conjugate 4	Distance (N3-C9)	Angle (N3-C9-C8b)
Match site	3.03 Å	150°
1 bp mismatch	3.12 Å	149°

✓ good proximity to the N3 to allow efficient alkylation

2024/1/25

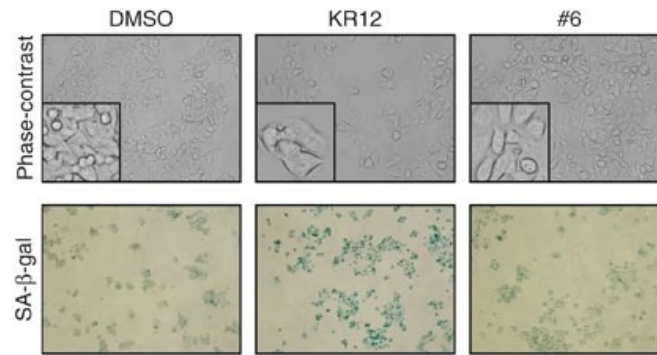
KR12 induced p53-dependent cellular senescence

Appendix (KR12)



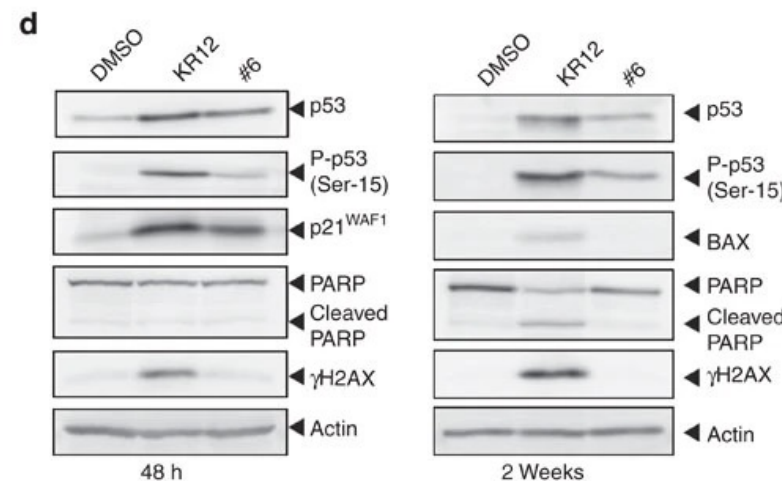
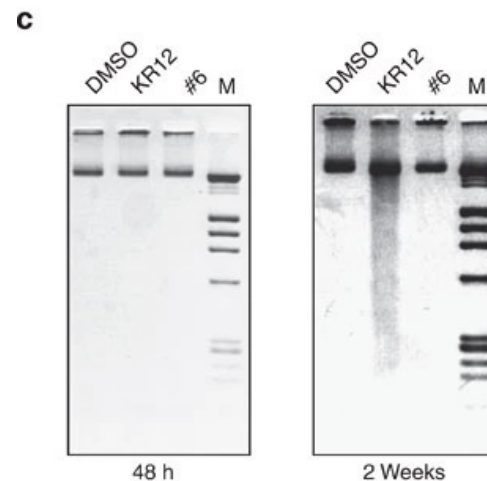
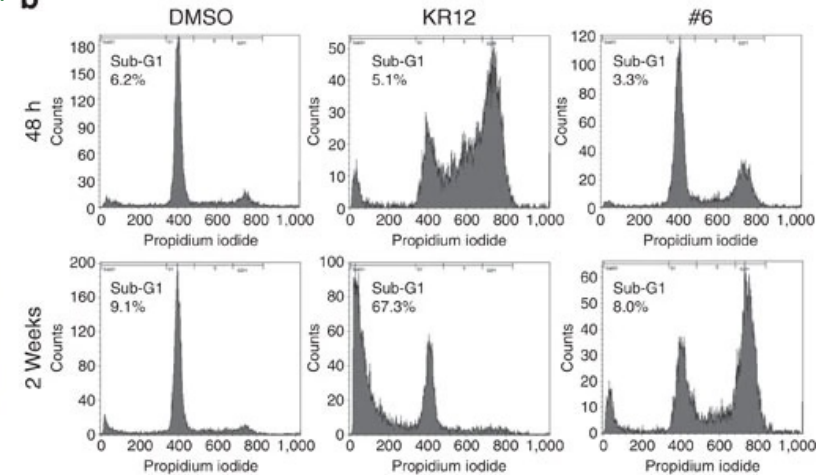
After KR12 treatment

- a flat cell morphology was displayed in LS180 cells
 - SA- β -gal activity was strongly increased
- KR12 induced cellular senescence



Cell cycle arrest

increase of the proportion of G2/M-phase cells



KR12 markedly induced phosphorylation of p53 at Ser-15, p21^{WAF1}/CIP1 and phosphorylated histone variant H2AX (γH2AX)

✓ KR12 promotes p53-dependent cellular senescence

2024/1/25

Effects of linker length of Bi-PIP and position of binding sites

Appendix (Bi-PIP)

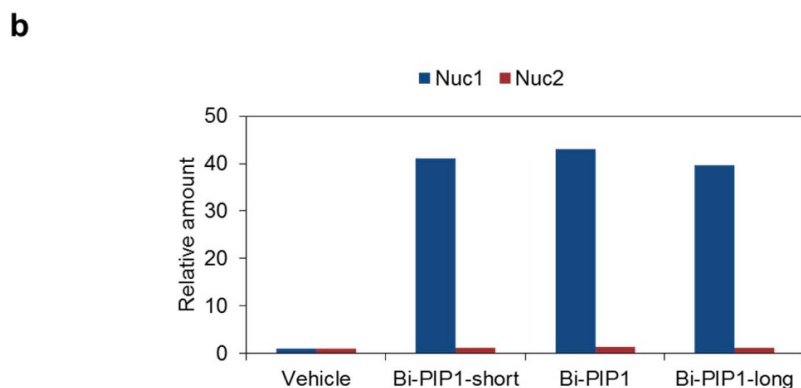
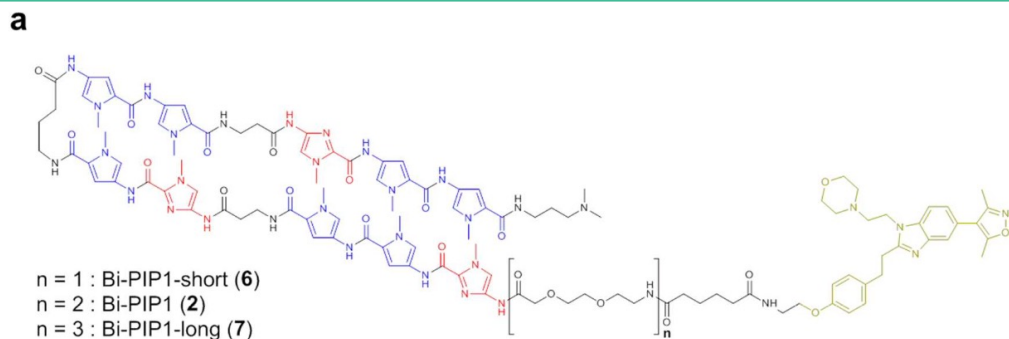


Fig.S4. Effects of the linker length.

(a) Chemical structure of Bi-PIP1-short (6) and Bi-PIP1-long (7). (b) A HAT reaction-*in vitro* ChIP-qPCR was performed for Bi-PIP1-short, Bi-PIP1 and Bi-PIP1-long with 10 nM of P300. Each compound was applied at a concentration of 100 nM.

- Effects of linker length of Bi-PIP sufficiently long and flexible linker for the effective acetylation of H3

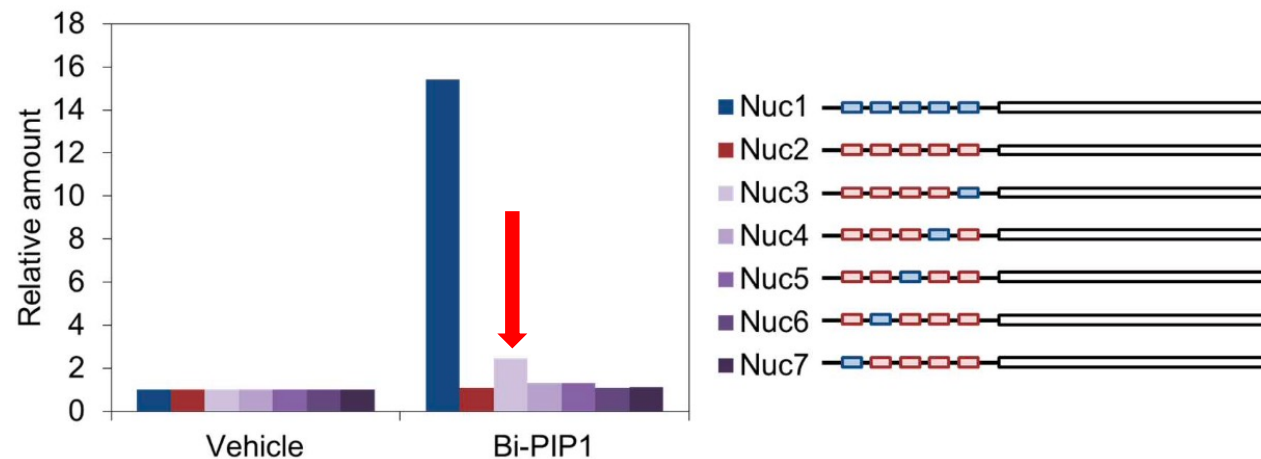


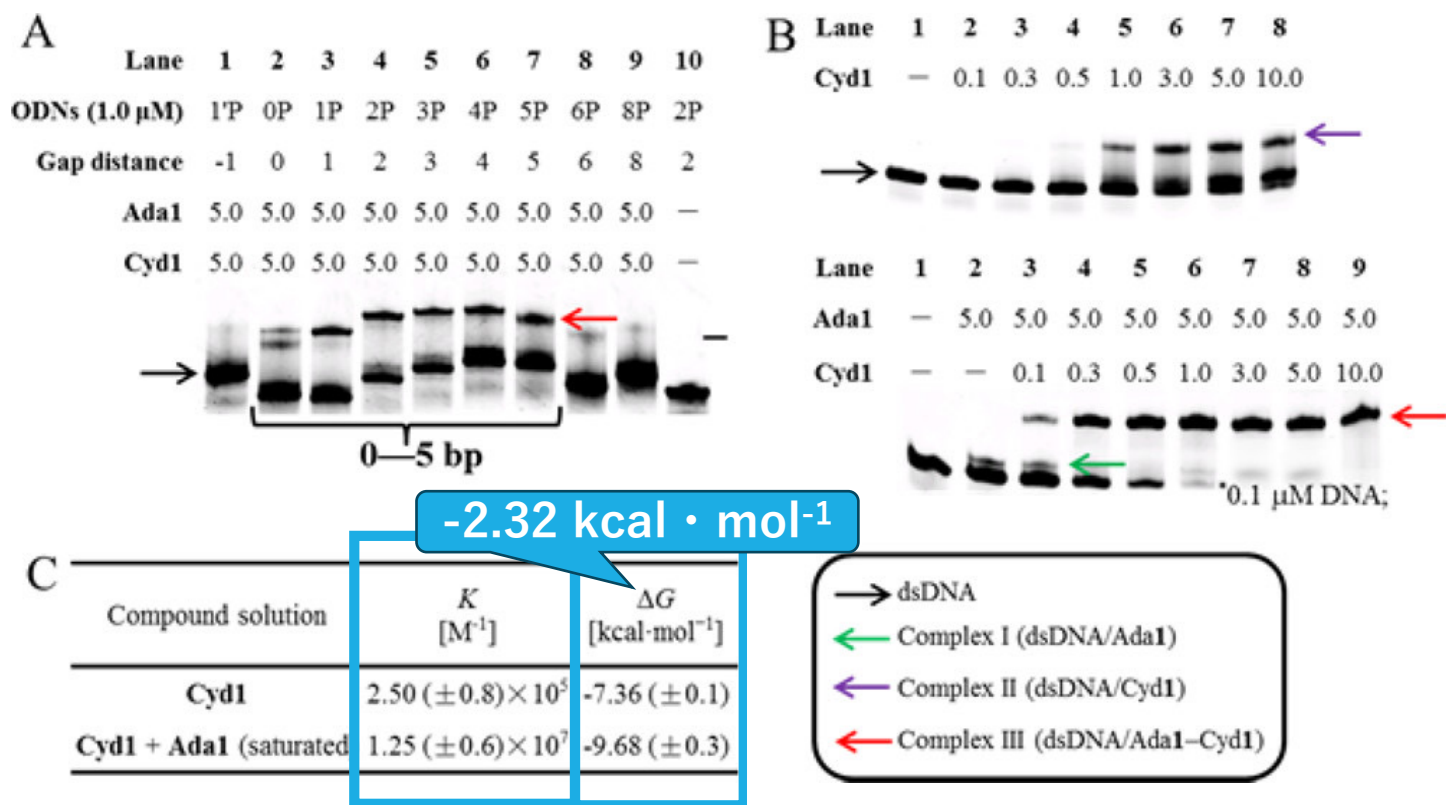
Fig.S5. Positional effects of the binding site.

A HAT reaction-*in vitro* ChIP-qPCR assay was performed for the mixture of seven nucleosomes (Nuc1–7, 10 nM each). 10 nM of P300 and 100 nM of Bi-PIP1 were used.

- Effective position for the acetylation
the sum of acetylation levels of Nuc3–7 \ll Nuc1
→ synergistic effects of multiple P300s on a single nucleosome

Pip-HoGu showed higher binding affinity

Appendix (PIP-HoGu)



EMSA (Gel Shift Assay)

Visualization of band shifts that form stable complexes

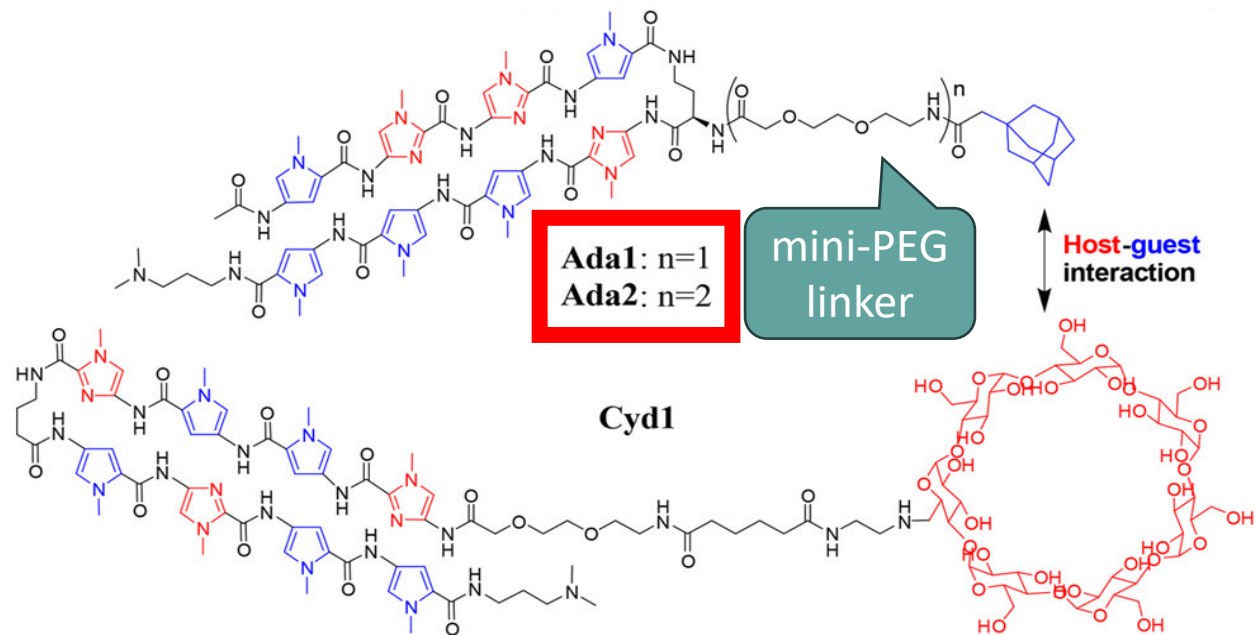
Figure 3. EMSA illustrating the cooperativity of Pip-HoGu. (A) The gel-shift behavior of all the positive ODNs with Ada1-Cyd1. Concentrations are shown in figure. (B) Quantitative EMSA of ODN2P with Cyd1 at various concentrations (top) and Cyd1 supplemented with saturated Ada1 (bottom). ODNs concentration: 0.1 μ M. (C) Equilibrium association constants and free energies for ODN2P with Ada1-Cyd1.

- ✓ Each bands can be distinguished.
- ✓ Cooperative binding was seen at 0-5 gap = Tm assay

2024/1/25

The cooperative energy of PIP-HoGu was highly distance dependent.

Appendix (PIP-HoGu)



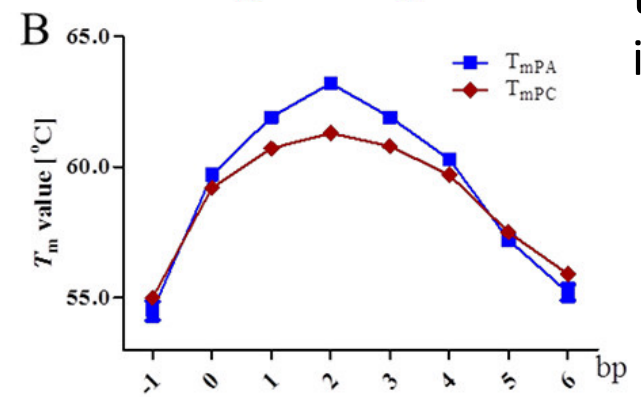
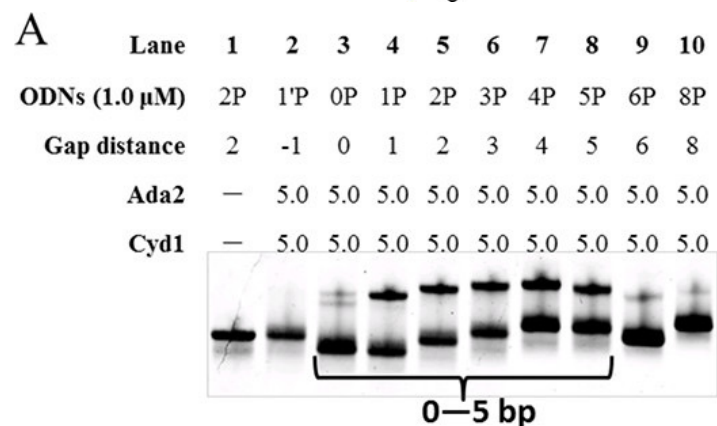
Influence of linker length on cooperative binding

Ada1 = 1 mini-PEG-linker

Ada2 = 2 mini-PEG-linkers

T_m Assay

- 0-4 bp gap → Ada2 showed lower stability than Ada1. (extra-long linker may destabilize the binding affinity)
- 5-6 bp gap → Ada2 showed slightly higher stability than Ada1. (longer and more flexible linker can make it easier to form complexes)



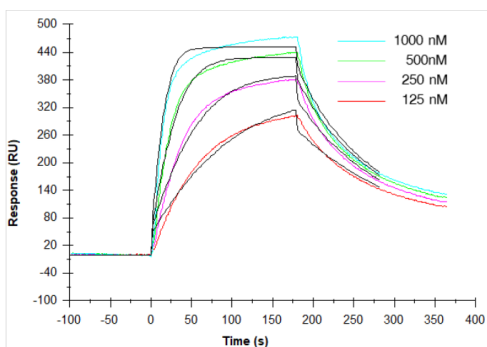
- ✓ The cooperative energy of PIP-HoGu is highly dependent on gap distances, and gap >5 bp will diminish the cooperation even if the linker length is long enough.

Figure 4. Mechanistic studies of cooperative binding. (A) The gel-shift behavior of all the positive ODNs with Ada2–Cyd1. (B) T_m profiles of all positive ODNs in the presence of Ada1–Cyd1 (T_{mPA} , blue, same as Figure 2B) and Ada2–Cyd1 (T_{mPC} , red).

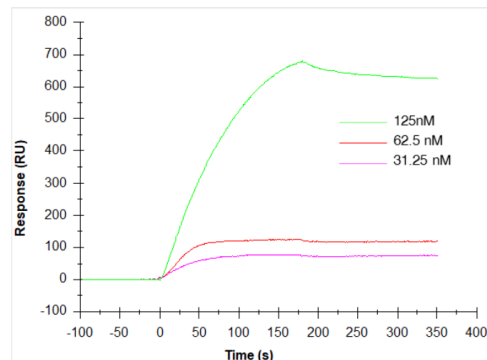
2024/1/25

Binding dynamics of Cuc1 and Ada3

B. SPR sensorgram of **Cyd1**



C. SPR sensorgram of **Cuc1**



D. SPR data in summary

Compound solution	k_a [$M^{-1}s^{-1}$]	k_b [s^{-1}]	K_D [M]
Cyd1	1.40×10^5	1.47×10^{-3}	1.05×10^{-7}
Cuc1	4.09×10^5	$< 7.49 \times 10^{-6}$	$< 1.83 \times 10^{-11}$

*Determined by fitting with a 1:1 binding model with mass transfer.

(B) SPR sensorgram of **Cyd1**. (C) SPR sensorgram of **Cuc1**. The sensorgrams were normalized to zero at the start point of injection, even though the interaction is irreversible. Thus, the accurate k_a of **Cuc1** can not be detected. (D) SPR data in summary. k_b of **Cuc1** was calculated based on a single injection (125 nM **Cuc1**) in a new chip. The concentrations were shown in figure. Extensive concentrations of **Cyd1** and **Cuc1** were dissolved in HBS-EP buffer (10 mM HEPES, pH 7.4, 150 mM NaCl, 3 mM EDTA, and 0.005 % surfactant P20) with 0.1% DMSO. These solutions were passed over a **Ada3**-biotinylated chip, in the absence of targeting DNA, immobilized on a sensor chip through a biotin-avidin system. Kinetic constants were calculated from the surface plasmon resonance sensorgrams for the interaction of guest conjugate **Ada**-PIP with host **Cyd**-PIP or **CB7**-PIP.

Appendix (ePIP-HoGu)

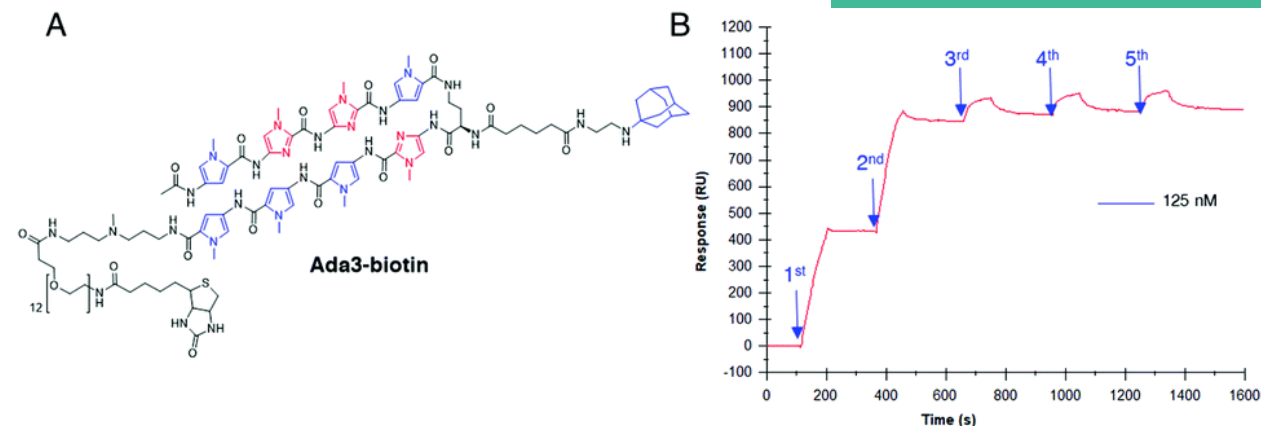


Fig. 3 (A and B) **Cuc1** binds **Ada3** irreversibly in the absence of DNA in an SPR assay. (A) Chemical structure of **Ada3**-biotin. (B) SPR sensorgram of **Cuc1** (125 nM) with multiple rounds of standard injection. One standard injection consisted of 180 s sample injection, followed by 180 s elution at $20 \mu L \text{ min}^{-1}$.

Surface plasmon resonance (SPR) assays

Cyd-assisted PIP-HoGu →

- ① the pair binding to DNA, ② the host-guest interaction or the procession of these two steps at a similar rate

CB7-assisted PIP-HoGu →

- ① binding the partner guest, ② synergic DNA binding

2024/1/25

Influence of spacing and binding orientation on cooperation

Appendix (ePIP-HoGu)

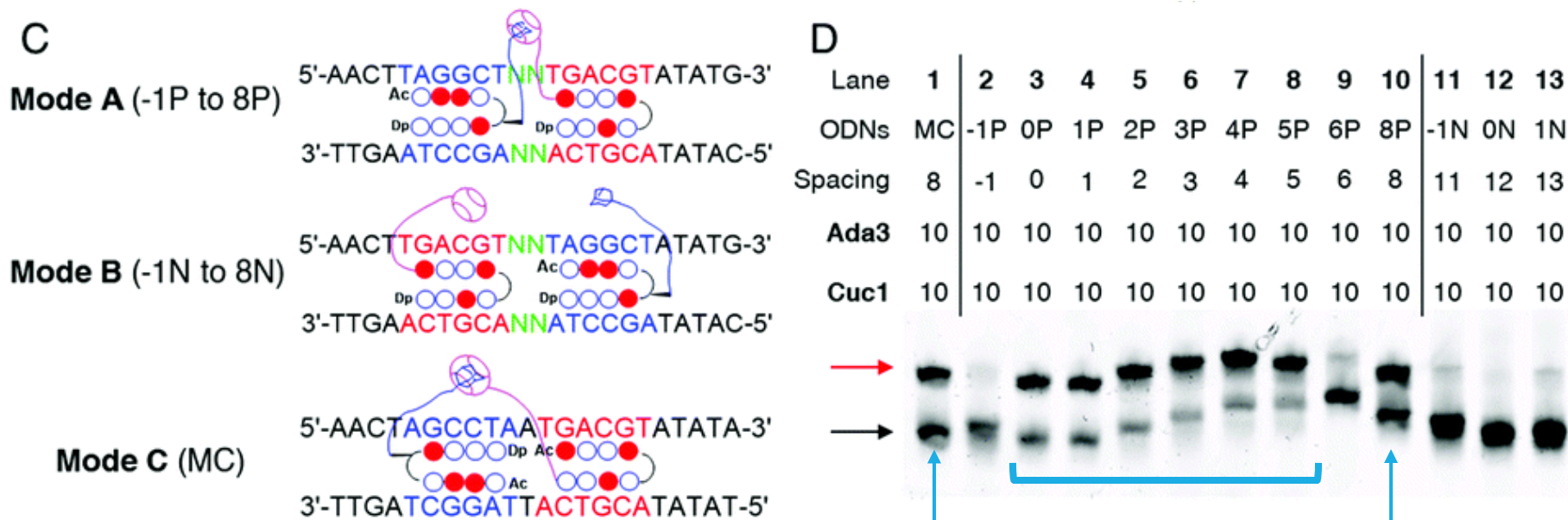


Fig. 3 (C and D) EMSA illustrating the cooperativity of the CB7-assisted DNA-binding system. (C) Three binding modes. Positive binding mode (Mode A) contains series dsDNA (-1P to 8P) with a gap distance (N) ranging from -1 to 8 bp. Similarly, negative binding mode (Mode B) includes dsDNA (-1N to 8N) with gap distance of -1 to 8 bp. (D) The gel-shift behavior of Modes A, B, and C with **Ada3-Cuc1**. ODN concentrations: 1.0 μ M. Compound concentrations: 10.0 μ M. Black arrow: ODNs. Red arrow: ODNs/Cuc1/Ada3.

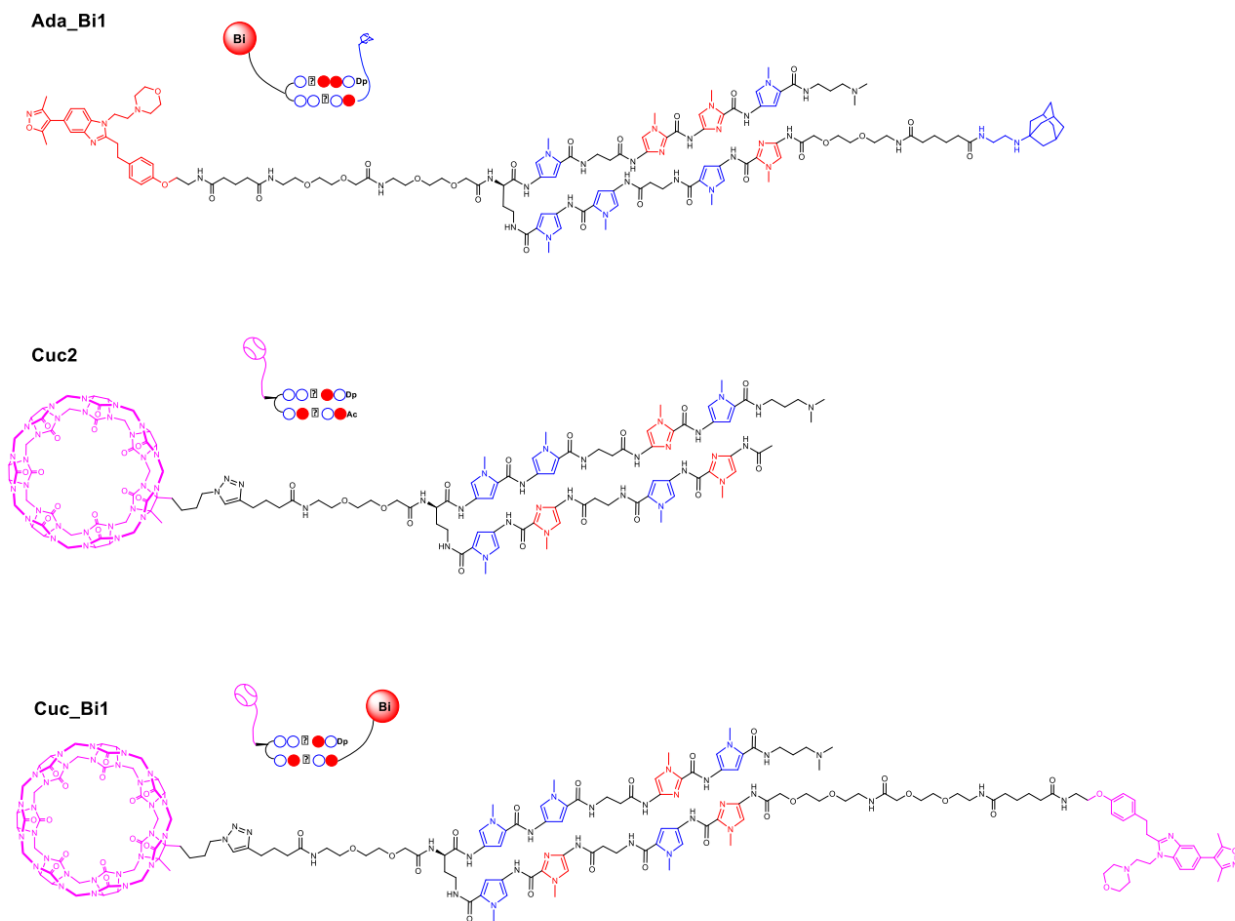
- EMSA (electrophoretic mobility shift assay) Cuc1-Ada3
 - 0-5 bp & 8 bp
 - 8 bp with partially reversed orientation
- a potent binding affinity

- The difference in band-shift with the spacings of 6 bp and 8 bp
- **DNA twist angle (host-guest moieties could meet through crossing the DNA major groove)**
 - distance between the two PIP-binding sites
 - linker length of the two conjugates

ePIP-HoGu showed high sequence-selectivity

Appendix (ePIP-HoGu)

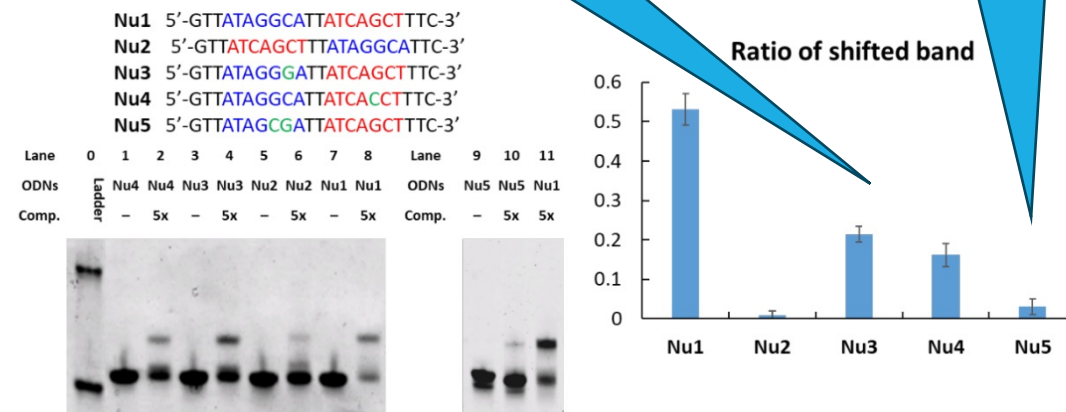
Figure S5. Chemical structures of conjugates used in HAT assay



>20 folds selectivity with 2 bp mismatch

2-3 folds selectivity with 1 bp mismatch

Figure S6. EMSA results of Ada_Bi1 + Cuc2 with four short dsDNA



The gel-shift behavior of **Ada_Bi1** + **Cuc2** with four kinds of ODNs: Nu1 to Nu4. ODNs concentration: 0.5 μ M. Compound concentration is 2.5 μ M. These short ODNs were inserted into nucleosome DNA strands. The ratio was calculated based on the equation of the intensity of shifted band \div (un-shifted band + shifted band). ODNs show only the forward DNA strand and omits the complementary DNA strand.

2024/1/25